W-AM-SymI-1 PRINCIPLES AND APPLICATIONS OF PULSED FIELD GEL ELECTROPHORESIS, Charles R. Cantor, Mathew K. Mathew, Guy Condemine, Stephanie Klco, and Cassandra L. Smith, Departments of Genetics & Development, Microbiology and Psychiatry, College of Physicians and Surgeons, Columbia University, New York, N.Y. 10032

A series of quantitative studies illustrates how PFG electrophoresis depends on such environmental variables as temperature, field strength, pulse time, gel porosity and field shape. These studies can be used to evaluate a number of different existing theoretical models of PFG. Most models can explain the bulk of the experimental observations but none can explain all of them. Even without a quantitatively satisfactory theory, PFG provides a powerful bird's eye view of the structure of whole chromosomes. This can be used to examine DNA rearrangements, patterns of DNA sequences, and higher order chromosome structure.

W-AM-SymI-2 HOW DOES PULSED-FIELD GEL ELECTROPHORESIS WORK? QUANTITATION OF THE SIEVING OF AGAROSE GELS. Philip Serwer, Gary A. Griess and Marjatta Son, Department of Biochemistry, The University of Texas Health Science Center, San Antonio, Texas 78284-7760.

During the agarose gel electrophoresis of DNA, length resolution is improved by periodically changing the direction of the electrical field applied. It has previously been assumed that viscoelastic relaxation of the DNA is the cause of this improvement. By use of a procedure for periodically rotating agarose gels during electrophoresis (rotating gel electrophoresis, or RGE), the dependence of length resolution on both temperature and the angle between two directions of the electrical field (ψ) suggest that viscoelastic relaxation of DNA is not a complete explanation. The observation that open circular DNA undergoes a voltage gradient-induced total arrest during agarose gel electrophoresis suggests that fibers protruding from agarose gels thread loops subtended from DNA random coils. Viscoelastic relaxation of these fibers, coupled to viscoelastic relaxation of the DNA, is a possible explanation of improved length resolution obtained by changing the direction of electrophoresis (tentatively referred to as the inverting lobster trap, or ILT, hypothesis). Preliminary studies of the separation of linear and circular molecules as a function of pulse time during field inversion gel electrophoresis (i.e., $\psi = 180°$) support the ILT hypothesis. RGE has been used to fractionate concatemers of bacteriophage T7 DNA produced during assembly of T7 in extracts of infected cells ("in vitro"). Bands produced by concatemers whose length is an integral (n) multiple of the length of monomeric T7 DNA (n as high as 15) were observed. Concatemers formed "in vitro" are potentially improved length markers for DNAs longer than 40 kb. Research performed in the authors' laboratory on RGE was supported by NIH (Grants GM24365 and AI22568).

W-AM-SymI-3 ORIENTATIONAL RELAXATION OF DNA IN AGAROSE GELS

Walter A. Baase, Daniel P. Moore and John A. Schellman
Institute of Molecular Biology, University of Oregon, Eugene, Oregon 97403

Large double-stranded DNAs, up to about 10 million basepairs, have recently been resolved in agarose gels by a technique which periodically changes the direction of the electric field. Though the mobility of long DNAs in agarose is approximately independent of molecular weight in a constant electric field, subjecting the system to pulsed fields which vary in direction or intensity leads to successful separations. While the phenomena are not completely understood, the overall mobility depends on the relaxation times for reorientation of the DNA molecules in the gel rather than on their steady state mobilities.

The measurement of the linear dichroism in the gel permits one to monitor the state of orientation of the DNA as a function of time. The procedure has the advantage that one can follow the instantaneous response of the DNA to abrupt changes in field direction or magnitude. Using a combined linear dichrometer-gel electrophoresis apparatus, we have measured the following relaxation processes for the DNAs of phages T7, T4 and G (40, 180 and 680 kbp, resp.): 1) orientation when the field is turned on, 2) disorientation when the field is turned off, 3) reorientation when the field is reversed, and 4) reorientation when the direction of the field is changed. None of these relaxation processes are simply exponential. Processes 1 and 3 are of unusual complexity and display unexpected oscillations about the eventual steady state. Our experimental results will be compared with the predictions of theoretical models.

We have also performed field reversal electrophoresis on the three DNAs under conditions comparable with the reorientation studies. We find that the field reversal interval that leads to a minimum in mobility is directly correlated with the time required to reach a minimum in the orientation function upon field reversal. (Supported by NSF Grant DMB-8609113 and PHS Grant GM-20195)

W-AM-SymI-4

SEQUENCE-DEPENDENT CURVATURE OF DNA

Paul J. Hagerman and Julia Promisel Cooper
Department of Biochemistry, Biophysics, and Genetics B-121
University of Colorado Health Sciences Center
4200 E. Ninth Ave. Denver, CO 80262 USA

Intrinsic, stable curvature of the helix axis of duplex DNA is now known to be a nearly ubiquitous phenomenon. In natural DNA, short runs of contiguous A residues [$(dA)_n$-$(dT)_n$; $n > 1$)] appear to be responsible for curvature, although the precise structural basis for curvature remains obscure. The hallmark of a curved DNA molecule is its reduced electrophoretic mobility (most pronounced on polyacrylamide gels) relative to DNA controls. Polyacrylamide gel electrophoresis has proven to be instrumental, not only for the discovery of curved DNA, but for its characterization as well. For example, we first demonstrated using synthetic DNA that macroscopic curvature is a consequence of the appropriate phasing of the oligo(dA)-oligo(dT) blocks [Hagerman, P. J., (1985) Biochemistry 24, 7033], as had been proposed earlier. More recently, we have examined the role of 5´-methyl groups on both C and T pyrimidines, and have found that, although curvature exists in the absence of such methyl groups, the degree of curvature is modulated by methyl groups in a position-dependent manner within the A/T block. We have also applied the electrophoretic approach to two related problems in DNA structure, namely, (1) the geometry of four-way DNA junctions and (2) the structural consequences of psoralen-crosslinking of DNA. These latter two problems will also be discussed.

W-AM-MinI-1 MECHANICAL TRANSDUCTION and STRETCH-ACTIVATED ION CHANNELS. Frederick Sachs, Biophysical Sciences, SUNY, Buffalo, N.Y. 14214.

Mechanical transduction serves a wide variety of functions at the systemic and cellular level. Touch, hearing, the sense of local gravity, and kinesthetic feedback from joints, tendons and muscles are systemic functions which depend upon specialized mechanical transducers. Mechanical feedback from the viscera provide the central nervous system with information necessary for the control of blood pressure and filling of the hollow organs as well as the homonal control of blood volume via the renin and ANF pathways. Mechanical transduction is necessary for the regulation of cell size and is undoubtedly fundamental in osmosensing. Stretch-activated (SA) channels are found in many organisms including E. Coli, yeast, higher plants, invertebrates and vertebrates and probably evolved as volume regulators. The channels vary in selectivity, but appear similar in the sensitivity to membrane tension and in density. The tension for half-activation ranges from 0.5-3 dyn/cm and densities are about $1/u^2$. The transduction model proposed by Guharay and Sachs (J. Physiol. 352, 685, 1984)-a channel linked in series with cytoskeletal strands and whose gating is controlled by channel strain energy- appears to be sufficient to explain mechanical transduction. The model predicts that maximal sensitivity to membrane tension occurs at a channel density in the range of $1/u^2$. Any sensitive, tension-activated, enzyme would have the same constraints on density and linkage to the cytoskeleton as the SA channels. The cytoskeletal strands in series with the channel may be fodrin (spectrin). Actin appears in parallel, reducing the sensitivity of the channels and because of its viscoelastic flow properties, causes slow sigmoidal channel activation in response to step changes in tension.---Supported by NIADDK DK37792 and USARO 22560-LS---

W-AM-MinI-2 Stretch-activated potassium channels in molluscan neurons and heart cells. Cathy Morris, Biology, U. of Ottawa, Ottawa, Canada, K1N6N5.

In the pond snail, Lymnaea stagnalis, neurons isolated from the CNS, and muscle cells of the ventricle invariably contain stretch-activated K^+ (SAK) channels at a density on the order of 1 per square micron. What could be the role of SAK channels in non-sensory cells? For a contractile cell they could provide a negative feedback for excitation-contraction coupling, but this would not explain their presence in neurons. Another possible role for such channels is to detect and remedy cell deformation produced by hypo-osmotic stress (HS). Lymnaea ventricle and kidney cells subjected to HS do not exhibit the volume regulatory decrease seen in some vertebrate cells, but they swell less than would be expected for a perfect osmometer. Swelling is more rapid and extensive in cells pretreated with quinidine (which blocks SAK channels) than in control HS. To assess the likelihood that limitation on swelling is induced by the initial swelling itself, we examined the efflux of Rb-86 from ventricle cells (having shown that rubidium is permeant in the SAK channel) under conditions of HS. Results are consistent with the hypothesis that swelling increases membrane permeability to Rb-86.

A look at neurons from a number of invertebrates indicates that the use of SAK channels may be more of a molluscan trait than a trait of, for example, freshwater invertebrates. We found that neurons of a terrestrial snail have SAK channels (and have preliminary evidence for a marine form), but the leech, a freshwater annelid, and the cockroach, an urban arthropod, gave no evidence of SAK channels. Supported by NSERC & MDAC.

W-AM-MinI-3 PRESSURE-SENSITIVE ION CHANNELS IN YEAST AND ESCHERICHIA COLI. B. Martinac, M.C. Gustin, X.L. Zhou, M.R. Culbertson, M. Buechner, A.H. Delcour, J. Adler, C. Kung (Intro. by Y. Saimi, Lab. of Molecular Biology, University of Wisconsin, Madison, WI 53706.

We have found pressure-sensitive ion channels in two microorganisms; in yeast Saccharomyces cerevisiae (Gustin, M.C. et al., Biophys. J., 51:251a, 1987) and in bacterium Escherichia coli (Martinac, B. et al., Proc. Natl. Acad. Sci. USA, 84, 2297-2301, 1987). Patch-clamp recording technique was used to study these channels in spheroplasts obtained from both microorganisms after enzymatic removal of the cell wall. The channels differed in several aspects from each other: 1. Two conducting states with conductances of 40 and 75 pS were recognized in yeast channels. The bacterial channels displayed a very large conductance of 970 pS with occasional appearance of conductance substates. 2. While the yeast channels preferentially passed mono- and divalent cations, the E. coli channels showed some preference for anions. 3. Besides being pressure-sensitive, the ion channels in E. coli spheroplasts were also voltage-dependent, showing higher opening probability upon membrane depolarization. Voltage had little effect on the pressure-activated channels in yeast. 4. Kinetically both channels differed in that the yeast channels gated on a millisecond time scale, while the bacterial channels gated on a second time scale. The function of pressure-sensitive ion channels in walled organisms is not known, but such channels may be involved in osmoregulation. Supported by NIH GM 37926 and DK 39121.

W-AM-MinI-4 MECHANICAL GATING OF TRANSDUCTION CHANNELS IN OTIC HAIR CELLS.

J. Howard and A. J. Hudspeth, Dept. of Physiology, Univ. of California, San Francisco, CA 94143-0444.

Mechanically sensitive channels located in the hair bundles of hair cells underlie the perception of sound and acceleration. Indirect experiments support a model for the gating of these transduction channels in which deflection of a hair bundle towards its taller stereocilia tenses elastic elements that pull directly on the channels. Because channel opening shortens the elastic elements, increased tension biases the channels to spend more time in their open state. A statistical-mechanical analysis of the model indicates that the stiffness of a bundle should be independent of displacement only when the channels are either all closed or all open; the stiffness should be smaller for intermediate positions and minimal when half the channels are open. The increased compliance of the bundle is analogous to the membrane capacitance contributed over a particular range of transmembrane potentials by the movement of the charged sensors of voltage-gated channels.

To detect the anticipated changes in bundle stiffness, we applied known forces *via* a flexible glass fiber to hair bundles from the bullfrog's sacculus. The resulting bundle displacements were measured optically while receptor potentials were recorded with glass microelectrodes. As predicted by the model, a bundle's stiffness, measured 2 ms after the onset of a force step, was minimal at bundle displacements for which roughly half of the channels opened. When a bundle was subjected to a static offset prior to stimulation, the relation between stiffness and displacement changed *pari passu* with that between receptor potential and displacement: the hair bundle's position of least stiffness changed as the transducer adapted. Gentamicin interferes with gating: bath application of this ototoxic drug at a concentration sufficient to block the transduction channels (100 μM) reversibly made the bundle's stiffness independent of position.

The magnitude of the stiffness deficit, 300 ± 100 $\mu N \cdot m^{-1}$, implies that each cell has 100 ± 50 transduction channels, each of which is opened by a force of 300 ± 100 fN ($\pm$ standard deviation, n = 24 cells). These estimates accord with those inferred from the simultaneously recorded receptor potentials. This research was supported by NIH grant NS20429.

W-AM-MinI-5 POSSIBLE ROLE OF ION CHANNELS IN STRETCH-INDUCED CONTRACTION OF SMOOTH MUSCLE.

Michael T. Kirber, John V. Walsh Jr., and Joshua J. Singer, Department of Physiology, University of Massachusetts Medical School, Worcester, MA 01655

As in many smooth muscle tissue preparations, single cells freshly dissociated from toad stomach, contract when stretched (Fay, INSERM 50:327, 1975). We have identified in these cells a stretch-activated channel which is most likely responsible for the initiation of this stretch-induced contraction (Biophys. J. 51:252a, 1987). Experimentally we induce stretch by applying suction to the patch pipette; raising the level of suction increases the probability that this channel will be found in an open state (P_O). This increase in P_O is due to a combination of decreased channel closed time durations and increased open time durations. The channel exhibits similar conductance to Na^+ and K^+ and less to Ca^{2+} and Ba^{2+}. With Na^+ or K^+ as the charge carrier (in the absence of Ca^{2+} at the extracellular surface of the channel) the channel exhibits inward-going rectification. The presence of normal Ca^{2+} (1.8 mM) in pipettes containing HEPES buffered physiological saline solutions decreases the unitary current and the slope conductance. Data obtained from patches containing many stretch-activated channels suggest that the channels in the same patch do not always respond identically to each other. The cell membrane is densely populated with this type of channel (1 channel per 3 um^2 at a minimum); thus, the excitatory influence of the population of these channels could dominate control of the membrane potential in response to mechanical stimulation. This channel may mediate stretch-induced contraction directly by conducting Ca^{2+} into the cell and/or indirectly by causing depolarization of the membrane and activating voltage sensitive Ca^{2+} channels. Supported by NSF DCB-8511674 and NIH DK-31620.

W-AM-MinI-6 ION CHANNEL ACTIVITY DURING OSMOREGULATION IN CLONAL NEUROBLASTOMA (N1E115) CELLS.
Lee Falke and Stanley Misler, The Jewish Hospital, St. Louis, Missouri.

N1E115 cells, like lymphocytes, erythrocytes, and epithelial cells osmoregulate; in hypotonic media they show rapid swelling and subsequent regulatory volume decreases (RVD). Ion channels might serve as stretch "sensors" or ion efflux "effector" pathways in this process. In cell attached patches (Ringers pipette) we now find that reduction of bath tonicity to 2/3-1/2 (by dilution of Ringers bath) provokes enhanced activity, at V_{rest}, of inward current pulses through 20-25 pS, stretch (i.e. pipette suction) activated, non-selective cation, C(SA), channels previously identified in ~60% of inside-out excised as well as cell attached patches (Falke, et al. Abst. Soc. Neurosc. 12 :47, 1986). The decline in C(SA) activity roughly parallels RVD, being much faster in 1/2 than 2/3 tonicity Ringers. During RVD, the cell is depolarized by $\gtrsim$ 10mV and at this new V_{rest} two other single channel currents are seen: (1) enhanced activity of outward current pulses through a 18 - 22pS delayed rectifier K+, K(DR), channel (Misler and Falke, Biophys.J.47 :146a, 1985) and (2) during rapid RVD, the onset of large, longlasting inward current pulses resembling those through a multiconductance state 200 - 350 pS anion channel seen in inside-out excised patches. We are currently testing the hypothesis that cell swelling ⟶ opening of C(SA) channels ⟶ both (1) menbrane depolarization ⟶ opening of K(DR) channels permitting K exit and (2) opening of higher threshold anion channels permitting Cl exit. In half tonicity Ringers these parallel processes may be present allowing cell volume to return to normal within 35 min.

W-AM-MinI-7 **STRETCH-ACTIVATED (SA) ION CHANNEL IN <u>XENOPUS</u> OOCYTES: PERMEATION AND BLOCK.**
X.C. Yang and F. Sachs, Dept. Biophysics, SUNY/Buffalo, NY

Our observations on permeation and block of SA-channel on cell-attached patches can be summarized as follows: (1) The current increases with extracellular potassium concentration according to Michaelis-Menten kinetics with a half saturation value of 153 mM and saturation current of 2.5 pA at zero membrane potential. (2) The current is a monotonic function of mole fraction in mixtures of lithium and potassium ions. These two results suggest that the oocyte SA-channel is a one-ion pore. The I-V curves are fitted well to two-barrier and one-site (2B1S) model with well of -2 kT and barriers 8.4 kT (outer) and 9.5 kT (inner) for K^+. (3) The current carried by monovalent cations has been observed in calcium free solution. (4) Calcium ions can go through SA-channel; in 160mM $CaCl_2$ the conductance is ca. 20 pS . (5) The current carried by sodium is reduced by millimolar calcium. The half-block concentration is ca. 1mM with weak if any voltage dependence. The dose response curve is well described by the 2B1S model with the two ion species competing for the same binding site. Calcium ions also produce a voltage independent shortening of the mean open time from 2-3 ms at zero calcium to 0.5 ms at 10 mM calcium. (6) Gadolinium (Gd^{3+}), one of the rare earth elements, blocks the SA-channel in a dose-dependent manner. The channel is completely blocked by 10 uM Gd^{3+}. Lanthanum (La^{3+}) also blocks the SA-channel but is less effective with ca. 100 uM required for complete blockade. Gd^{3+} blocks geotropism in plant roots (B.G. Pickard, personal communication). Since plants express SA-channels (Biophys. J.51,251a), these observations suggest that SA-channel may play a role in gravity sensing in plants. **Supported by NIADDK DK37792 and USARO 22560-LS.**

W-AM-MinII-1 STRUCTURES INVOLVED IN THE DOCKING OF CYTOCHROME C AND ELECTRON TRANSFER IN REACTION CENTERS OF RHODOBACTER SPHAEROIDES. D.M. Tiede*, C.-H. Chang+, O. El-Kabbani*, J. Tang*, M.R. Wasielewski*, J.R. Norris* and M. Schiffer+, *Chemistry Division and +Division of Biological and Medical Research, Argonne National Laboratory, Argonne, Illinois, 60439.

A striking feature of Rb sphaeroides and Rps viridis reaction centers is that both the L and M protein subunits and the chromophores are arranged with approximate two-fold symmetry, yet normal photochemistry does not follow this approx. symmetry. We have examined the protein environment surrounding the pigments in the Rb sphaeroides R-26 structure, and found a set of differences in the amino acid residues at symmetry related positions on the L and M subunits. Comparison with the Rps capsulata and viridis sequences shows that this set of differences is conserved in each. This set of residues includes differences between L146/M173, L97/M124, L181/M208, L104/M131, L210/M250. We suggest that these residues may contribute to the selectivity of electron transfer. A model for Rb sphaeroides cyt c_2-RC complex has also been built, based upon dichroism observed for this complex and a complimentary pairing of charges on each protein. Charged residues on the RC periplasmic surface are not symmetrically distributed. Instead, a "patch" of charged residues is found which we propose to be the cyt binding site. This site is composed predominantly of residues on the surface ab helix (M86,M87,M94,M99,M109) and the L-terminus (L257,L261,L268), but also involves M182, M290, L155. A Rb sphaeroides cyt c_2 model is found to dock on this site, stabilized by at least 11 salt bridges between complimentary charges on the cyt and RC surfaces. This model accounts for the optical dichroism observed for the cyt c_2-RC complex. Significantly, this model includes salt bridges formed between the RC and asp 93, lys 95, lys 97 on cyt c_2, which are part of a 10 amino acid insert present in cyt c_2 but absent in cyt c. The different dichroism seen for the cyt c-RC complex can be explained by the absence of this segment in the cyt c. The model predicts that the orientation of cyt bound to the RC can be controlled by the distribution of charge residues on the cytochrome surface.

W-AM-MinII-2 STRUCTURAL AND THEORETICAL MODELS FOR REACTION CENTER (BACTERIO)CHLOROPHYLLS. K.M. Barkigia, L. Chantranupong, L.K. Hanson, M.A. Thompson, M.C. Zerner and J. Fajer. Brookhaven National Laboratory, Upton, New York 11973.

a) INDO/s calculations of bacteriochlorophyll (BChl) dimers predict optical shifts, relative to BChl monomers, comparable to those observed experimentally for the special pair primary donors in bacterial reaction centers (R.C.). b) The significant optical differences observed in R.C.'s containing different BChl chromophores: 960 nm for the first transition in Rps. viridis, comprised of BChls b, and 870nm in Rb. sphaeroides, composed of BChls a, are not accounted for by exchanging BChl a and b, although recent x-ray data show that the two organisms maintain a common donor architecture. However, shifts of that magnitude are calculated if the interplanar spacing between the two macrocycles of the dimer is changed by 0.2-0.3Å, in accord with crystallographic results (Deisenhofer et al., Allen et al., Schiffer et al.). c) For bacteria containing BChl a, variations of 0.1Å or less can account for the range of absorption maxima between 870 and 840 nm observed in different organisms. d) Crystallographic data for a crowded porphyrin (Zn tetraphenyl-octaethyl porphyrin) show the macrocycle to be severely puckered. The first optical transitions are significantly red-shifted and the molecule is easier to oxidize than other Zn porphyrins. MO calculations predict the experimental trends and indicate that the structural deformation destabilizes the highest occupied orbital. Similar optical and oxidation trends are predicted for puckered chlorins and bacteriochlorins, and raise the intriguing possibility that conformational differences within the special pairs, such as are actually observed in Rps. viridis, modulate redox properties and thereby help control the direction of electron flow at the onset of charge separation in the R.C. (Work supported by the U.S. Department of Energy.)

W-AM-MinII-3 PICOSECOND STUDIES OF ELECTRON TRANSFER INVOLVING CHLOROPHYLLS. M.R. Wasielewski and D.G. Johnson, Chemistry Division, Argonne National Laboratory, Argonne, IL 60439.

Recent theoretical studies and photochemical hole-burning experiments have suggested that formation of an intramolecular charge transfer state involving the two bacteriochlorophyll molecules of the special pair dimer occurs following photon absorption. We have explored this possibility in symmetric, fixed distance chlorophyll dimer in which the macrocycles share a common vinyl group at the 2-position. We have found that this dimer exhibits a remarkable decrease in fluorescence quantum yield as the medium dielectric constant increases. This decrease is accompanied by a proportional decrease in the lowest excited singlet state lifetime as measured by picosecond fluorescence and absorption. For example, the singlet state lifetime of the dimer in toluene (ϵ = 2.4) is 2.5 ns, while that in butyronitrile (ϵ = 20) is 0.31 ns. The decrease in excited state lifetime is attributed to the formation of a mixed state containing substantial charge transfer character. This state then decays non-radiatively.

We have measured the rates of oxidation of the lowest excited singlet state of chlorophyll by a quinone and the rates of the subsequent radical ion pair recombination reaction by picosecond spectroscopy in a series of fixed-distance chlorophyll-quinone molecules. The overall dependence of the rates on free energy of reaction follow the Marcus prediction of decreasing rate for highly exergonic reactions. The results show that ultrafast rates of electron transfer are easily achieved for moderate exergonicities in chlorophyll containing donor-acceptor molecules.

Work performed under USDOE contract W-31-109-Eng-38.

W-AM-MinII-4 THE FUNCTION OF SPECIFIC AMINO ACID RESIDUES IN THE REACTION CENTER OF *Rhodobacter capsulatus*. Edward J. Bylina, William J. Coleman and Douglas C. Youvan, Department of Applied Biological Sciences, Massachusetts Intstitute of Technology, Cambridge, MA 02139 U.S.A.

The bacterial photosynthetic reaction center is the first integral membrane protein whose structure has been determined to atomic resolution. To further investigate the relationship between the protein structure and the function of the complex, we have substituted specific amino acid residues on the L and M subunits by site-directed mutagenesis in *R. capsulatus*. Single-site mutants containing amino acid replacements in several key chromophore/cofactor binding sites have been constructed using M13 phage and other engineered bacterial vectors. The mutations include sites involving the L and M special-pair bacteriochlorophyll (BChl), voyeur BChl and bacteriopheophytin, as well as the primary and secondary quinones (Q_A and Q_B) and the non-heme iron. We have carried out preliminary characterization of reaction centers isolated from these mutants, using spectroscopy, photosynthetic growth assays and other analytical methods. The results of these studies have enabled us to begin to evaluate the role of specific protein residues in the function of the bacterial reaction center.

W-AM-MinII-5 THE STEP WHICH REQUIRES CALCIUM IN PHOTOSYNTHETIC OXYGEN EVOLUTION IS THE S_3 TO S_0 TRANSITION. A. Boussac and A.W. Rutherford. Service de Biophysique, CEN/Saclay 91191 Gif-sur-Yvette cedex, France

Oxidation of water by Photosystem-II requires the storage of four positive charges on its donor side. The charge storage states are designated S_0 to S_4. Oxygen is release during the S_4 to S_0 transition. The loss in activity after the release of the 18 and 24 KDa proteins by NaCl-washing in the light can be restored by addition of Ca^{2+}. The step at which the system is inhibited in the absence of Ca^{2+} is under debate. Thus we have studied the yield of the S_2-state formation by monitoring its characteristic EPR multiline signal at helium temperature, after each flash of a sequence fired at room temperature. After one flash, the S_2-state was present in the same amount with and without Ca^{2+}. In the presence of Ca^{2+} the amplitude of the multiline signal oscillated with a period 4 while in the absence of Ca^{2+} the oscillatory pattern corresponded to an inhibition occuring at the S_3 to S_0 transition. Complications due to the possible occurence of flash-induced Ca^{2+} release during the course of the experiment can be discounted on the basis of the following observations : 1) In Ca^{2+} deficient material the S_2-state deactivated via the S_2 multiline state. 2) Continuous pre-illumination had little effect on the amplitude of the S_2 multiline signal when photoinduced after a period of dark adaptation. These results contradict earlier EPR studies in which Ca^{2+} depletion was reported to inhibit S_2 multiline formation. This effect may be at least partially due to the presence of high concentrations of EGTA in the samples used in some of the earlier work. We have observed that EGTA is able to quench the multiline signal. This effect is apparently unrelated to the inhibitory effect of Ca^{2+} depletion.

W-AM-MinII-6 TYROSYL RADICAL INVOLVEMENT IN THE PHOTOSYNTHETIC OXYGEN-EVOLVING SYSTEM. B.A. Barry, R.J. Debus, I.D. Rodriguez, L. McIntosh and G.T. Babcock, Department of Chemistry and the Plant Research Laboratory, Michigan State University, East Lansing, MI 48824.

By using functional aromatic amino acid anxotrophs of cyanobacteria, the tyrosine residues in these species may be deuterium labelled. When this is done with perdeuterated tyrosine, the EPR spectrum of D^{+}, a free radical species associated with the water-splitting reactions in Photosystem II, narrows substantially. Based on this result and additional work with specifically deuterated tyrosines, we assign the D^{+} species as a tyrosine radical with significant unpaired electron spin density at the 1, 3 and 5 ring carbon positions. ENDOR spectroscopy of this radical is consistent with these conclusions and has provided the principal hyperfine tensor components for several of the protons in the radical. Site specific mutagenesis of tyr^{160} in the D-2 polypeptide of the PSII core identifies this residue as the specific tyrosine responsible for the EPR spectrum. Analogous experiments are underway to identify the Z^{+} radical in PSII. (Supported by the USDA CRGO Photosynthesis Program, by NIH GM 37300 and by the McKnight Program.)

W-AM-A1 ELECTRON MICROSCOPIC CHARACTERIZATION OF THE ALPHA CRYSTALLIN ELUTION PEAK AFTER GEL FILTRATION. Jane F. Koretz, Center for Biophysics and Biology Dept., RPI, Troy, NY 12180-3590, and Robert C. Augusteyn, Biochemistry Dept., Univ. of Melbourne, Parkville 3052, Victoria.

Alpha-crystallin, the major protein component of vertebrate eye lenses, is eluted from a gel filtration column as a single very broad peak beginning in or shortly behind the void volume. The breadth of this peak is consistent with in vivo light-scattering studies which are interpreted as a heterogeneous population of molecular weights from about 500 kDa to 1500 kDa. To determine the size, shape, and heterogeneity of the alpha-crystallin aggregate population by direct visualization of the particles, fractions were taken across the peak, cross-linked with gluteraldehyde, and examined in the electron microscope. The smallest particles were about 7 nm, smaller than reconstituted alpha-crystallin aggregates, and increased in diameter linearly up to about 13.5 nm. Beyond this size, the aggregates appeared to elongate into rods/chains whose average length increased across the elution peak. The largest fractions (those closest to the void volume) exhibited the longest rod/chains, as well as some indication of "sheets" whose appearance is similar to that of hydrostatic pressure-induced disks but larger and more irregular. The variability in size and shape of these aggregates is similar to that observed in studies of organic amphiphiles in polar solvent, and consistent with the idea that alpha-crystallin will aggregate into micellar types of structures (cf. Augusteyn and Koretz, FEBS Letters, 1987).

Supported in part by grant EY02195 from NIH.

W-AM-A2 HYDROSTATIC PRESSURE-INDUCED CHANGES IN THE AGGREGATE ORGANIZATION OF ALPHA-CRYSTALLIN. Jane F. Koretz, Center for Biophysics and Biology Dept., RPI, Troy, NY 12180-3590, and Robert C. Augusteyn, Biochemistry Dept., Univ. of Melbourne, Parkville 3052, Victoria (Intr. by J. V. Landau)

Alpha-crystallin, the major protein of the lenses of vertebrate eyes, appears to be an amphiphilic molecule, according to hydrophobicity analysis of the amino acid sequence. This factor, combined with evidence that all the subunits are in identical microenvironments and the numerous conflicting reports of aggregate size/molecular weight, led us to propose that alpha-crystallin aggregates into micellar structures (FEBS Letters, 1987), the first such naturally occurring example in proteins. If true, then application of increased hydrostatic pressure to alpha-crystallin particles should result in an increase in turbidity while under pressure and, possibly, an alteration of the aggregate form. We have found a 5.5-fold turbidity increase upon application of 2000 psi hydrostatic pressure to a 0.5 mg/ml solution of 9-10 nm diameter alpha-crystalline aggregates. Electron microscopic examination of samples after exposure to increased hydrostatic pressure and release shows an organizational change from the small spheres to what appear to be disks of significantly increased diameter. These results are consistent with the micelle hypothesis. Of equal interest, disk-like structures can also be observed in crude preparations from the lens.

Supported in part by grant EY02195 from NIH.

W-AM-A3 THERMAL DENATURATION OF CHROMATIN AT HIGH SALT CONCENTRATIONS. M.R. Riehm, LCP, NIADDK, National Institutes of Health, Bethesda, MD 20205 and R.E. Harrington, Department of Biochemistry, University of Nevada, Reno, NV 89557

The interactions which stabilize chromatin structure are thought to be primarily electrostatic and hydrophobic in nature. Accordingly, at salt concentrations above approximately 75mM sodium, which includes the physiological region, extensive interfiber aggregation occurs in solution which has limited previous spectroscopic and thermal denaturation studies on the dynamics of chromatin unfolding in this ionic strength domain. We have developed techniques in which high molecular weight polyacrylamide suspensions are used to limit fiber diffusion and thus minimize chromatin aggregation at salt concentrations up to and above 600 mM sodium. Low percentage highly crosslinked polyacrylamide gels just above the critical point in the chemically polymerized sol to gel transition are used to generate critical point sols by mechanical disruption and mild heating. Chromatin samples mixed with these sols induce the sol to gel transition in a process of complex coacervation. In this state, salt insoluble chicken erythrocyte chromatin is stabilized against large scale aggregation and precipitation during thermal denaturation at high sodium ion concentrations. The hyperchromic effect in DNA melting in these systems is reproducible and consistent throughout a wide range of sodium concentrations. Empirical spectroscopic techniques are discussed which isolate temperature-dependent hyperchromic signals at 260 nm due to conformational changes in the chromatin DNA and **quasi**-hyperchromic effects due to local environmental changes which promote anomalous light scattering.

W-AM-A4 AN ANALYSIS OF THE P22PROCAPSID LIKE PARTICLES ASSEMBLED FROM PURIFIED PROTEIN SUBUNITS.
Peter E. Prevelige, Jr., Dennis R. Thomas & Jonathan King. Dept. of Biology, MIT, Cambridge, MA 02139.

The closed double shelled procapsids of the bacteriophage P22 can be assembled in vitro from purified protein subunits. The assembly process requires the presence of both the coat and scaffolding proteins. When the proteins were mixed together they rapidly ($t_{1/2}$ = 5 min.) and efficiently (up to 90%) polymerized into particles that are morphologically similar to procapsids. The kinetics of the assembly process were dependent upon the scaffolding and coat protein concentrations. In vivo the scaffolding to coat protein ratio is tightly regulated at the translational level. Varying the ratio of the scaffolding protein to coat protein in vivo has yielded information about the assembly reaction. At excess scaffolding protein the procapsids incorporated scaffolding protein up to the sterically enforced limit of 300 molecules. At limiting scaffolding protein the procapsids incorporated approximately 140 molecules of scaffolding protein. Intermediate values were not observed. The particle diameter was dependent upon the amount of scaffolding present in the assembly reaction.

The minor proteins, gp16 and gp20, when present in the reaction mixture were also incorporated in the newly assembled procapsids. These proteins are thought to be involved in the DNA process. Preliminary evidence suggests that the presence of these proteins in vitro results in an increase in the rate and efficiency of assembly.

W-AM-A5 RECONSTRUCTION OF PARTICLES WITH VARIABLE PITCH.
Bridget Carragher, David A. Bluemke, Robert Josephs.
Department of Molecular Genetics and Cell Biology, University of Chicago, Chicago, IL.

In the reconstruction of helical particles, it is normally assumed that translation along the length of a particle is coupled to rotation about its axis. This assumption is not valid for particles whose pitch varies along the particle length (eg. actin, HbS fibers), and application of these algorithms results in significant errors in the reconstructed density map. We have developed an iterative procedure for reconstructing particles with variable pitch. In this procedure the local pitch of the particle is estimated and incorporated into the reconstruction algorithm. The local pitch is derived from a cross-correlation analysis between the variable pitch particles and a trial model having constant pitch. The constant pitch models are constructed using coordinates measured from the reconstructed density maps. Each iteration of the procedure provides an improved estimate of the pitch which is incorporated into the succeeding iteration. The fidelity of the reconstruction is determined from cross-correlation between the original micrograph and a ***variable*** pitch model. The iterations are continued until the cross-correlation coefficient between the variable pitch model and the micrograph of the particle is maximized.

The iterative procedure has been evaluated using model structures which incorporate variations in pitch similar to those actually occurring in sickle hemoglobin fibers. The results indicate that the iterative reconstruction procedure considerably reduces the errors associated with constant pitch reconstructions. These tests provide a basis for applying this procedure in the structural analysis of micrographs of helical particles which display variable pitch.

This work has been supported by NIH grants HL 30121 and HL 22654 (RJ) and GM07281 (DAB).

W-AM-A6 ON THE STABILITY OF SICKLE HEMOGLOBIN MACROFIBERS.
B.L. Gabriel, T. Lee, R. Josephs. Dept. of Molecular Genetics and Cell Biology, University of Chicago, Chicago, IL.

Macrofibers and crystals of sickle hemoglobin are composed of structural units called double strands arranged in rows or layers. Within a row the double strands have the same orientation and in adjacent rows they have opposite orientations. In crystals the double strands are linear whereas in macrofibers they twist gently about the particle axis with a 10,000 Å periodicity. Six-row macrofibers are composed of 6 rows (or layers) containing 10-12 double strands per row. The double strands are axially displaced from their crystalline positions. We have observed 6 row macrofibers in which two rows are peeling from the particle, leaving a four-row macrofiber. The peeled sections, called 2-row laminae, resemble twisted ribbons with alternating wide and narrow regions having diameters of 475 ± 70 Å and 190 ± 20 Å, respectively. The distance between narrow regions is 4875 ± 750 Å. The wide region has unit cell dimensions of 64 x 53 Å and a density distribution which corresponds to the ac face of the HbS crystal. The origin and structure of the 2-row laminae confirm earlier structural studies showing that macrofibers are composed of layers of double strands. The laminae arise because the strength of the bonding vectors within a row of double strands is greater than the strength of contacts between rows. These observations can account for the disorder between rows of double strands seen in macrofibers and paracrystals.

This work has been supported by NIH Grant HL22654 and HL30121 Project II.

W-AM-A7 NEW STRUCTURAL FEATURES IN THE BASAL BODY OF THE BACTERIAL FLAGELLUM REVEALED BY LOW DOSE MICROSCOPY AND IMAGE ENHANCEMENT. G.E. Sosinsky, N.R. Francis, M.J.B. Stallmeyer and D.J. DeRosier. Brandeis University, Waltham, MA 02254.

The bacterial flagellum is powered by a rotary motor of which the basal body is an important component. Low dose images of negatively stained whole and partially disassembled basal bodies from Salmonella typhimurium were averaged by single particle averaging methods. The hook-basal body (HBB) complex consists of the hook which connects the motor to the filament, a rod extending from the end of the hook, and four rings (denoted L, P, S, and M) through which the rod passes. The rings are associated with the cell envelope: the M ring with the inner membrane, and the L ring with the outer membrane. The intermediate structures found upon incubation at pH 4.0 were the hook and rod with the L and P rings but no S or M ring (denoted HLPR); hook with the L and P ring but no extending rod (HLP); individual rings; and structures resembling staples, which are thought to be the L-P complex. At pH 4, these intermediates are stable, with the HBB and HLPR being the predominant structures. Fine structural details not seen under high dose conditions are present in averages of low dose images. An extra feature, a ridge, between the L and P rings, also seen in Caulobacter crescentus basal bodies, is evident in the averages of all structures containing L and P rings. By comparing HLP, HLPR, and HBB averages, the rod is seen extending from the base of the P ring, passing through the S ring, and stopping just short of the end of the M ring. The rod has a knob on the M-S end. From the averaged images, we computed three-dimensional maps of the cylindrically averaged structures. These maps show that the M ring appears to be unconnnected to the rod while the S ring sits on the knob of the rod. In cross-section, the L ring is shaped like the Greek letter Π, the two arms of the Π forming the ridge.

W-AM-A8 THREE-DIMENSIONAL ARCHITECTURE OF THE ESCHERICHIA COLI RIBOSOME. T. Wagenknecht, M. Radermacher, J.M. Carazo, A. Verschoor, M. Boublik* and J. Frank, Wadsworth Center for Laboratories and Research, New York State Department of Health, Albany, New York 12201 and Roche Institute of Molecular Biology, Roche Research Center, Nutley, New Jersey 07110.*

Recently a new technique of three-dimensional image reconstruction, which does not require crystalline specimens, was applied to electron micrographs of negatively stained large ribosomal subunits (Radermacher et al., EMBO J. 6:1107, 1987). The major new structural feature of the reconstruction was a deep groove (~16 nm length X 4-5 nm maximal width X 6 nm maximal depth) extending across the subunit just below its central protuberance and on the side which binds the small ribosomal subunit to form the ribosome. This groove is termed the "interface canyon" (IC).

Additional evidence for the existence and potential functional significance of the IC is provided by three-dimensional reconstructions of the complete ribosome and of the large subunit selectively depleted of the stalk-forming proteins, L7/L12. Interestingly, in the ribosome about half of the canyon is exposed and appears well-suited to bind at least two tRNA molecules in a configuration that makes good biochemical and structural sense. The absence of the L7/L12 proteins, which in the native subunit are located near one terminus of the IC, apparently causes some structural rearrangements in this region of the canyon as well as in more distal locations, which could account for the diverse effects of the removal of these proteins on ribosomal function. Finally, the possibility that the IC is an artifact caused by positive staining of rRNA has been ruled out by analysis of electron micrographs of unstained frozen-hydrated large ribosomal subunits. Supported by NIH grant 1R01 GM29169.

W-AM-A9 THREE-DIMENSIONAL STRUCTURE OF ROTAVIRUS BY CRYO ELECTRON MICROSCOPY. B.V.V. Prasad, G.J. Wang, J.P.M. Clerx and W. Chiu. Dept. of Biochem., Univ. of Arizona, Tucson, AZ 85721.

Rotaviruses, major pathogens of infantile gastroenteritis in humans and animals, are double shelled with an additional inner core encapsidating the genomic dsRNA. We have determined the three-dimensional structures of double- and single-shelled simian rotavirus at 40Å resolution by image processing the electron images of unstained virus particles embedded in a thin layer of vitreous ice. Our studies show that both the outer and the inner shells have T=13 icosahedral surface lattice. The double-shelled virion has a smooth outer surface with 60 slender spikes extending outwards. The protein mass is distributed uniformly on the local and strict 2- and 3-fold axes. A plausible interpretation is that the spikes belong to the minor protein VP3 and rest of the outer surface is occupied by the major protein VP7. The protein volume in the outer shell is consistent with 60 VP3 and 780 VP7 molecules. A striking feature in the structures of both double- and single-shelled virions is the presence of large aqueous channels at all the 5- and 6-coordinated positions. The outer and the inner shells interact such that their channels coincide linking the outer surface and the inner core. It is suggested that these channels may provide pathways for the metabolites required for the RNA transcription to reach the parental templates and for the newly synthesized mRNA molecules to exit from the transcriptionally active single-shelled particles. Single-shelled virion exhibits a bristly surface. The protein mass is mainly concentrated on the local and strict 3-fold axes suggesting a trimeric clustering. The 260 morphological units at all the local and strict 3-fold axes are interpreted to represent 260 trimers of VP6, the major protein of the single-shelled virion. This inference is further supported by computer image analysis of 2-d crystalline arrays of VP6 which strongly indicate trimeric clustering.

W-AM-A10 STRUCTURE DETERMINATION OF FILAMENTOUS BACTERIOPHAGE PF1 BY X-RAY AND NEUTRON DIFFRACTION

Wilhelm Stark, Raman Nambudripad and Lee Makowski
Dept. Biochemistry & Molecular Biophysics, Columbia Univ. P&S, New York, NY 10032.

The filamentous bacteriophage Pf1 consists of a large number of identical, 46 residue, protein subunits helically arranged around a circular single-stranded DNA molecule forming a rod approximately 65Å in diameter and 1.9 long. The structure of the coat protein is being studied using X-ray and neutron diffraction from magnetically oriented specimens. Neutron diffraction data from native and valine deuterated specimens were collected to about 8Å resolution in the equatorial and 13Å in the meridional direction. These data were used to locate the five valine residues relative to the alpha-helices of the coat protein. These positions indicated that the helical surface lattice is right-handed and that the two alpha-helical segments run parallel to each other. X-ray fiber diffraction data have been collected to about 3.5Å resolution. Molecular models for the Pf1 coat protein are being refined against the X-ray data using restrained least-squares refinement. Three models are currently being refined. One of them uses a right-handed surface lattice and another a left-handed one. The third uses both the symmetry and residue positions determined by neutron diffraction. Comparison of the results of the independent refinements will allow an assessment of the refinement procedure for use with fiber diffraction data. The results of these refinements should provide a detailed description of the structure of the viral protein coat at 3.5Å resolution.

W-AM-A11 THE CRYSTALLOGRAPHIC STRUCTURE OF A PLANT VIRUS RELATED TO MAMMALIAN PICORNAVIRUSES.

Cynthia Stauffacher, Ramakrishnan Usha, Tim Schmidt, Yunge Li, Melissa Harrington and Jack Johnson, Department of Biological Sciences, Purdue University, West Lafayette, Indiana 47907.

Cowpea mosaic virus (CpMV) is the type member of the comoviruses, a group of positive strand RNA viruses which share many physical and biological properties with mammalian picornaviruses such as human rhinovirus, poliovirus and hepatitis A virus. The crystallographic structure of this virus was undertaken to show how these similarities might be expressed in the capsid structure. Comoviruses are icosahedral viruses with T=1 symmetry, containing sixty copies each of two polypeptides, 42kD and 24kD in molecular weight. Picornaviruses also have T=1 symmetry, but contain four types of capsid proteins, three with molecular weight in the range 25-35kD and one small 7kD protein. Alignment of the RNA from CpMV and picornaviruses shows homology in the nonstructural viral genes, but none in the capsid proteins, although they occur in the same relative position in the genome. The crystallographic structure of this virus has been solved to 3Å resolution using techniques of phase extension and real space averaging. The electron density map at 3Å shows a quartenary and tertiary structure for CpMV remarkably similar to the picornaviruses, with three β barrels arranged in a pseudo T=3 symmetry. Details of the surface structure differ, reflecting the differences in the viral hosts. Stabilization of the capsid of CpMV also differs because of the structural requirements of two versus three major capsid proteins in these two viral types. Comparisons of the similarities and differences in these capsid structures may not only indicate where the viruses have adapted to their hosts, but may also reveal some clues to virus evolution.

W-AM-B1 **The Ca^{2+}-gated Ca^{2+} channel is localized in the junctional sarcoplasmic reticulum of skeletal muscle.** Francesco ZORZATO and Pompeo VOLPE. *Istituto di Patologia Generale dell'Universita' di Padova, via Loredan 16, 35100 Padova, Italy*

Muscle contraction is triggered by the release of Ca^{2+} from terminal cisternae (TC). TC are composed of two different, yet continuous types of membranes: Ca^{2+} pump and junctional face membrane (JFM). A protein of 350 kDa has been identified as a component of the junctional feet, which connect transverse tubules (TT) to sarcoplasmic reticulum (Kawamoto, R. M., Brunschwig, J. P., Kim, K. C., and Caswell, A. H. (1986) J. Cell Biol. 103: 1405-1414). Doxorubicin induces Ca^{2+} release from isolated TC by opening Ca^{2+} channels (Zorzato, F., Salviati, G., Facchinetti, T., and Volpe, P. (1985) J. Biol. Chem. 260: 7349-7355). It is not known whether the Ca^{2+} channels are distributed uniformely over th TC membrane area. The localization of Ca^{2+} channels was revealed by studying the effect of anti-(JFM) antibodies (Ab) and anti-(350 kDa protein) affinity purified polyclonal Ab on doxorubicin-induced Ca^{2+} release from TC of rabbit skeletal muscle. Upon preincubation of the TC with anti-(JFM) and anti-(350 kDa protein) Ab the initial rate of doxorubicin-induced Ca^{2+} release was inhibited by 50% at an Ab/TC ratio of 1. Ca^{2+}-dependent ATPase and Ca^{2+}-loading rates were unaffected by anti-(JFM) Ab, whereas the anti-(350 kDa protein) Ab had a stimulatory (25%) and inhibitory (50%) effect on each function, respectively. It was also found that doxorubicin-induced Ca^{2+} release from isolated TC was Ca^{2+} dependent with maximal rates around 1 uM free [Ca^{2+}]. These results indicate that doxorubicin-induced Ca^{2+} release is mediated by Ca^{2+}-gated Ca^{2+} channels which are selectively localized in the junctional face membrane of TC and are likely involved in excitation-contraction coupling.

W-AM-B2 **CALMODULIN-DEPENDENT PHOSPHORYLATION OF SARCOPLASMIC RETICULUM (SR) INHIBITS Ca^{2+} RELEASE INDUCED BY SEVERAL Ca^{2+} RELEASE TRIGGERING METHODS.** Do Han Kim Dept. of Medicine, University of Connecticut Health Center, Farmington, CT 06032.

To test the hypothesis that calmodulin-dependent phosphorylation of the 60 kDa protein regulates various types of Ca^{2+} release, the efflux time course of passively-loaded $^{45}Ca^{2+}$ was measured by rapid filtration after addition of various Ca^{2+} release solutions to phosphorylated and non-phosphorylated Ca^{2+}-loaded SR. The initial rapid Ca^{2+} release triggered by 2 μM Ca^{2+}, 2 mM caffeine, 50 μM quercetin or 50 μM doxorubicin was completely inhibited by phosphorylation of the 60 kDa protein (15 pmol P/mg SR) regardless of the triggering methods. Subsequent, slower Ca^{2+} release after addition of each of the Ca^{2+} release triggering solutions to phosphorylated SR, revealed that Ca^{2+} release was partially resumed following an initial 1 - 4 s lag period. The time course of the resumed Ca^{2+} release from phosphorylated SR depended on the drug used. Estimation of the rates of dephosphorylation of the 60 kDa protein, determined by dilution of the [^{32}P]-labeled protein with each of the Ca^{2+} release solutions followed by SDS gel electrophoresis, suggests that the rate of dephosphorylation of the 60 kDa protein was highest in the presence of 50 μM quercetin which is consistent with the finding that inhibition of quercetin-induced Ca^{2+} release by phosphorylation is rapidly reversed upon further filtration. These findings indicate that the phosphoprotein inhibits all of these types of Ca^{2+} release. Supported by NIH grant HL 33026.

W-AM-B3 **IDENTIFICATION OF Ca^{2+} RELEASE PROTEINS IN CARDIAC SARCOPLASMIC RETICULUM (SR) USING DOXORUBICIN AS A PHOTOAFFINITY LABELING PROBE.** Do Han Kim, Young Sup Lee and Arnorld M. Katz. Dept. of Medicine, University of Connecticut Health Center, Farmington, CT 06032.

Doxorubicin, an anticancer drug has been reported to induce Ca^{2+} release in skeletal muscle sarcoplasmic reticulum (SR) and photoaffinity labeling by ^{14}C-doxorubicin used to identify the putative Ca^{2+} release proteins. In an attempt to identify Ca^{2+} release proteins in canine cardiac SR, we have examined Ca^{2+} release time course of actively-loaded junctional cardiac SR by double-wavelength spectrophotometry using antipyrylazo III as an extravesicular Ca^{2+} indicator. Ca^{2+} release was found to be triggered by 50 - 100 μM doxorubicin and the doxorubicin-induced Ca^{2+} release inhibited by 1 μM ruthenium red. Under experimental conditions used for the Ca^{2+} release assay, cardiac SR was photoaffinity labeled with ^{14}C-doxorubicin by irradiation with long wavelength ultra-violet light. The major site of doxorubicin binding was on a 36 kDa protein, approximately 11 pmol ^{14}C-doxorubicin being incorporated by 1 mg SR. Three additional doxorubicin binding proteins (350 k, 110 k and 60 kDa) with lower extents of incorporation were also identified. The hypothesis that the 36 kDa doxorubicin binding protein is a Ca^{2+} release protein was tested further by examining the effect of caffeine or ruthenium red on the doxorubicin binding to the 36 kDa protein. Addition of 2 mM caffeine inhibited doxorubicin binding by approximately 36 %, whereas 1 μM ruthenium red inhibited doxorubicin binding by 53 %. These findings are consistent with the hypothesis that the 36 kDa protein may play an important role in the Ca^{2+} release mechanism. Supported by NIH grant HL 33026.

W-AM-B4 HIGH MOLECULAR WEIGHT (HMW) PROTEINS FROM CANINE CARDIAC JUNCTIONAL SARCOPLASMIC RETICULUM VESICLES (JSRV) ARE THE RYANODINE (RY)-SENSITIVE CALCIUM RELEASE CHANNEL.
David P. Rardon, Robert D. Mitchell, Steven M. Seiler, Dominic C. Cefali, and Larry R. Jones. From the Krannert Institute of Cardiology, I.U. School of Medicine, Indianapolis, IN 46202.

We were the first to show that Ryanodine (RY) dramatically stimulates ATP-dependent Ca uptake by JSRV (Jones, L.R., and Cala, S.E. J. Biol. Chem. 256:11,809, 1981). HMW proteins, putative components of the SR Ca release channel, were purified to homogeneity from cardiac JSRV and fused with planar lipid bilayers to elucidate the mechanism of RY action. HMW proteins were partially purified from Zwittergent 3-14 solubilized JSRV using gel filtration chromatography. Zwittergent 3-14 was exchanged with CHAPS by sucrose gradient centrifugation, yielding a 305/320 kDa protein doublet purified to apparent homogeneity. When purified HMW proteins were fused with planar bilayers (cis: 2.5 uM CaC12, 125 mM Tris, 250 mM HEPES; trans: 50 mM Ba(OH)2, 250 mM HEPES), single channel activity was observed with a mean channel amplitude of 6 pA at 0 mV. The channel had a mean slope conductance of approximately 80 pS which was identical to that observed with native cardiac JSRV. 1 mM cis ATP prolonged channel open time; however, channel opening was inhibited with 1 mM cis (referable to the cytoplasmic face) EGTA (1 nM free Ca). RY at low concentrations (1 nM) substantially increased the percentage of time that the channel was in the open state, whereas micromolar RY (40 uM) effectively inhibited channel open time. These data strongly suggest that RY-induced blockage of the large Ca channel in JSRV accounts for the stimulation of ATP-dependent Ca uptake measured with micromolar RY and that cardiac HMW proteins are integral components of the RY-sensitive, Ca-induced Ca release channel of the SR membrane.

W-AM-B5 SPECTROSCOPIC ANALYSIS OF CARDIAC PHOSPHOLAMBAN (PLB). Heather K.B. Simmerman, D. Eugene Lovelace, and Larry R. Jones. From the Krannert Institute of Cardiology and the Department of Medicine, Indiana University School of Medicine, Indianapolis, Indiana 46202.

The structure of PLB, a phosphorylatable protein associated with cardiac sarcoplasmic reticulum, was probed by using ultraviolet absorbance, intrinsic fluorescence, and far ultraviolet circular dichroism (CD) spectroscopy. Purified PLB was examined in three detergents: octyl glucoside, n-dodecyl octaethylene glycol monoether ($C_{12}E_8$), and sodium dodecyl sulfate (SDS). The ultraviolet absorption and intrinsic fluorescence spectra reflected the aromatic amino acid composition of PLB, and no significant differences were observed between samples of dephosphorylated PLB and PLB which had been phosphorylated by the catalytic subunit of cAMP-dependent protein kinase. Ultraviolet CD spectroscopy in the range 250-190 nm demonstrated that PLB possesses a very high content of alpha-helix in all three detergents and is unusually resistant to denaturation. For samples in SDS, no change in the CD signal was observed after boiling the protein to dissociate the subunits, suggesting that the high helical content of PLB is not a result of subunit oligomerization. Phosphorylation did not significantly change the secondary structure of PLB. A two-domain model of PLB is proposed in which each domain contains a stable helix and phosphorylation may rotate one helix relative to the other.

W-AM-B6 **REACTIVE DISULFIDE COMPOUNDS TRIGGER Ca^{2+} RELEASE FROM SARCOPLASMIC RETICULUM (SR) VESICLES.** G. Salama, N.F. Zaidi, J.J. Abramson* and C. Lagenaur†, University of Pittsburgh School of Medicine, Department of Physiology and Neurobiology†, Pittsburgh, PA 15261 and *Portland State University, Department of Physics, Portland, OR 97207.

Reactive disulfide compounds like 2,2' dithiodipyridine (DTDP), 4,4' dithiodipyridine, N-succinimidyl 3(2-pyridyl) dithiopropionate (SPDP) etc., trigger Ca^{2+} release from SR vesicles isolated from rabbit skeletal muscle that were actively loaded using an ATP regenerating system. Release was observed with compounds containing a pyridyl ring adjacent to a disulfide and the kinetics of Ca^{2+} release was correlated with the generation of thiopyridone in the reaction mixture; measured as ΔA at 340 nm. Reactive disulfides oxidize free SH groups by exchanging the SH with a thiol in the disulfide bond, resulting in the production of a new disulfide bond and a thiopyridone. Thus, the oxidation of SH groups on SR protein(s) and the formation of disulfide bonds with the exogenously added reagent elicits Ca^{2+} release from the SR. Subsequent additions of reducing agent dithiothreitol (DTT, 1 mM) reversed the effect and resulted in a rapid re-uptake of the released Ca^{2+}. The disulfides and DTT had no effect on Ca^{2+} transport driven by the Ca^{2+}, Mg^{2+}-ATPase. Ca^{2+}-release induced by DTDP was inhibited by ATP or ADP; Mg^{2+} and cAMP in the range of 0.25 to 1 mM produced a slight stimulation, but greater concentrations inhibited Ca^{2+} release. In skinned rabbit psoas fibers, DTDP elicited rapid twitches which were blocked by ruthenium red. The results show that the oxidation reduction of a free SH group on an SR protein regulates the opening and closing of a Ca^{2+} channel, which is not the ATPase. Supported by AHA grants 87915 to J.J.A., 871065 to G.S., the Western Pennsylvania, and Oregon affiliates of the AHA, an RCDA to G.S. J.J.A. is an Established Investigator of the AHA.

W-AM-B7 TOPOGRAPHY OF THE Ca-ATPase POLYPEPTIDE OF SARCOPLASMIC RETICULUM. Terrence L. Scott, Boston Biomed. Res. Inst. and Dept. of Biol. Chemistry, Harvard Med. School, Boston, MA 02114.
The primary structure of the Ca-ATPase polypeptide of SR has been deduced from its cDNA and a model for its tertiary structure and folding pattern within and through the bilayer has been proposed (Brandl, et al., Cell, 44, 597, 1986). The proposed structure has been investigated using fluorescence quenching and fluorescence energy transfer measurements. The distances between various donor-acceptor pairs including analogs bound at the nucleotide site (FITC, TNP-ATP), Ca sites (lanthanides), covalent probes (IAEDANS, Ca-dependent carbodiimide incorporation) and probes located in the bilayer have been determined. Consideration of these distances and resulting triangulation indicates inconsistencies in the proposed tertiary structure of the ATPase. The measured distances in conjunction with covalent probe localization in the amino acid sequence yield a low resolution map of the ATPase tertiary structure. Supported by grants from NIH, NSF and an Established Investigatorship of AHA.

W-AM-B8 ROLE OF CALSEQUESTRIN IN THE REGULATION OF CA^{2+} RELEASE FROM SARCOPLASMIC RETICULUM Noriaki Ikemoto[a,b], and Makoto Koshita[c] a Dept. Muscle Res., Boston Biomed. Res. Inst., Boston, Mass. 02114; b Dept. Neurol., Harvard Med. Sch.; c Dept. Physiol., Nagoya City Univ. Med. Sch., Nagoya, Japan

We studied the correlation between the process of development of Ca^{2+} release and the time course of Ca^{2+} uptake. The time course of Ca^{2+} uptake (viz. an increase in the sum of bound and free Ca_i) that was monitored by a chemical quench technique or spectrometry with arsenazo III was at least biphasic (k_1=0.7-2.5 s^{-1}; k_2=0.02-0.10 s^{-1}), while an increase in the free $[Ca^{2+}]_i$ monitored by chlorotetracycline fluorescence paralled the slow phase. Therefore, the rapid phase represents primarily a rapid binding of the transported Ca^{2+} to the internal binding sites, probably to calsequestrin. The amount of Ca^{2+} released by caffeine, which was determined at various times of Ca^{2+} uptake, increased in parallel to the internal binding rather than the increase of $[Ca^{2+}]_i$. Upon rapid increase of $[Ca^{2+}]$ from ~0 to ≥0.25 mM, conditions that would occur in the vesicle during the rapid phase of Ca^{2+} uptake, tryptophan fluorescence of the isolated calsequestrin increased first at k=2.8-4.0 s^{-1} and then at k=0.1-0.28 s^{-1}. The Ca^{2+}-induced fluorescence changes were completely inhibited by ruthenium red (e.g. 2 uM). These results suggest a hypothesis that the rapid conformational changes of calsequestrin occurring in the initial phase of Ca^{2+} uptake affect the Ca^{2+} release channels, making them ready to open upon triggering. (Supported by grants from NIH and MDA)

W-AM-B9 PHOSPHODIESTERASE INHIBITORS AND PHOSPHORYLATION OF SARCOPLASMIC RETICULUM AND MYOFILAMENTS IN INTACT MYOCARDIUM. S.T. Rapundalo*, R.J. Solaro+, and E.G. Kranias*, Depts. of Pharmacology and Cell Biophysics*, and Physiology and Biophysics+, University of Cincinnati, Cincinnati, OH 45267

The influence of selective (milrinone, MIL) and non-selective (isobutylmethylxanthine, IBMX) phosphodiesterase inhibitors and β-adrenergic agonists (isoproterenol, ISO) on phospholamban and myofibrillar phosphorylation was studied in guinea pig hearts perfused with [^{32}P]-orthophosphate. Changes in protein phosphorylation were compared to alterations in tissue cAMP levels and positive inotropic effects induced by these agents. ISO (0.01 μM), MIL (50 μM), and IBMX (100 μM) all produced similar, two-fold increases, in left ventricular +dP/dt but only IBMX and ISO were associated with significant increases in phospholamban phosphorylation. At these equipotent doses, the effects of IBMX were associated with higher increases (3.1-fold) in cAMP than those observed with ISO (2-fold). MIL (50 μM) produced a 2.5-fold increase in cAMP levels, but failed to change phospholamban phosphorylation. Higher doses of MIL (100 μM) resulted in relatively high (4.1-fold) cAMP levels and this was associated with increased (1.5-fold) phosphorylation of phospholamban. Phosphorylation of TnI was significantly increased at 0.01 μM and 0.1 μM ISO while phosphorylation of C-protein was only observed at 0.1 μM ISO. IBMX and MIL did not significantly increase phosphorylation of either TnI or C-protein at any of the doses studied. These findings indicate that cardiotonic agents acting via the cAMP pathway may produce similar inotropic responses at different levels of cAMP, and phosphorylation of sarcoplasmic reticulum and myofibrillar proteins. (Supported by NIH Grants HL22619, HL26057, HL22231.)

W-AM-B10 PERMEABILITY AND GATING PROPERTIES OF THE PURIFIED RYANODINE RECEPTOR-CALCIUM RELEASE CHANNEL FROM SKELETAL MUSCLE SARCOPLASMIC RETICULUM. Jeffrey S. Smith‡, Toshiaki Imagawa*, Kevin P. Campbell* and Roberto Coronado‡. Dept. of Physiology and Molecular Biophysics‡, Baylor College of Medicine, Houston, TX 77030 and Dept. of Physiology and Biophysics*, University of Iowa, Iowa City, IA 52242.

The ryanodine receptor of rabbit skeletal muscle sarcoplasmic reticulum was purified from CHAPS soluble triads by immunoaffinity chromatography as a single 450,000 Da polypeptide. The purified receptor had a [^{3}H] ryanodine binding capacity (B_{max}) of 490 pmol/mg and a binding affinity (K_d) of 7.0 nM. Using planar bilayer techniques we show that the purified receptor forms monovalent and divalent-selective channels. Ryanodine receptor channels were identical to calcium release channels described in native sarcoplasmic reticulum. In the present work, four criteria were used to establish this identity, i) activation of channels by micromolar Ca^{2+} and millimolar ATP, and inhibition by micromolar ruthenium red, ii) a main channel conductance of 110 ± 10 pS in 54 mM trans Ca^{2+}, iii) a long-term open state of lower unitary conductance (40 ± 2 pS and 22 ± 3 pS) induced by micromolar ryanodine, and iv) a permeability ratio P_{Ca}/P_{Tris} of 11 to 14. In addition, we show that the purified ryanodine receptor channel displays a saturable conductance in both monovalent and divalent cation solutions (γ_{max} for K^+ = 1 nS and γ_{max} for Ca^{2+} = 172 pS). In the absence of Ca^{2+} channels had a broad selectivity for monovalent cations but in the presence of Ca^{2+}, they were selectively permeable to Ca^{2+} against K^+ by a permeability ratio P_{Ca}^{2+}/P_K^+ = 6.6. Receptor channels displayed 4 conductance levels and from this we propose that the intact calcium release channel is a tetramer of tightly coupled equivalent channel subunits.

W-AM-C1 MACROSCOPIC NA^+ CURRENTS IN INTACT VENTRICULAR HEART MUSCLE MEASURED WITH THE LOOSE PATCH VOLTAGE CLAMP METHOD. Richard E. Weiss, Dept. of Pediatrics, UCLA, Los Angeles, CA 90024-1743.

The loose patch voltage clamp method (Stühmer, Roberts, & Almers in Single Channel Recording, eds. Sakmann & Neher, Plenum, 1983) was used to measure macroscopic sodium currents from the surface of papillary muscles from the right ventricles of rats and guinea pigs. This method makes possible the measurement of fast ionic currents in an intact, syncytial preparation with sub-millisecond resolution. Muscles were superfused during dissections and in the experimental chamber with a phosphate-buffered Krebs-Ringer solution, saturated with a 95% O_2, 5% CO_2 gas mixture. Patch pipettes were filled with the same (ungassed) solution. Due to the average cardiac cell diameter of 10 - 20 µm, pipettes of less than 12 µm tip diameter were used. At 26^o - 27^o C, inward currents first appeared in response to depolarizing pulses of appoximately 30 mV (relative to the intrinsic cell resting potential). Maximum inward currents were elicited by depolarizing pulses of 60 - 70 mV. Standard H-infinity plots showed half-inactivation occurred at slightly hyperpolarized membrane potentials indicating that appreciable resting inactivation is present. Currents were reversibly blocked by TTX. Potassium currents were also recorded and, in the presence of TTX, were measurable with little delay (< 1 ms) from the onset of the pulse. (Supported by a Grant-in-Aid from the American Heart Association with funds contributed by the California Affiliate, and a Laubisch Award.)

W-AM-C2 VOLTAGE CLAMP STUDY OF NA/CA EXCHANGE IN CULTURED CHICK HEART CELL AGGREGATES. J.R. Stimers and M. Lieberman, Dept. Physiology, Duke University Medical Center, Durham, NC 27710.

Our laboratory has previously demonstrated the electrogenicity of Na/Ca exchange in cultured cardiac cells (Jacob et al. J. Physiol. 387:567,1987). In frog atrial myocytes, Hume and Uehara (J. Gen. Physiol. 87:857, 1986) attributed "creep current" to Na/Ca exchange activity. We have used a single electrode switching voltage clamp to identify and characterize similar membrane currents in cultured heart cell aggregates (80-130 µm in diameter) under control conditions and after Na-loading by 3 µM monensin (Na/H ionophore). Depolarizing the membrane from a holding potential of -80 mV to various potentials reveals that a slowly decaying outward creep current is augmented by the Na-load. Returning to -80 mV elicits a slowly decaying inward creep current which increases in magnitude with both the duration and potential of the prior pulse. These currents are completely blocked by addition of 20 mM Mn to the perfusate but are not blocked by 200 µM Cd. The instantaneous IV relations following a step from -80 to 0 mV of either 50 or 300 ms duration are nearly linear but tend to saturate at both positive and negative potentials. Increasing the prepulse duration causes the IV relation to shift downward and change the reversal potential by about +15 mV. We also find that the reversal potential shifts to more positive potentials with increasing depolarization during the prepulse. The characteristics of the above current are consistent with its resulting from stimulation of Na/Ca exchange by the elevation of Na_i and the Ca_i accumulation during the voltage clamp pulses. Supported by NIH grants HL27105, HL17670 and HL07101.

W-AM-C3 α_1-ADRENERGIC AND MUSCARINIC RECEPTOR-MEDIATED CHANGES IN INTRACELLULAR CA^{2+} CONCENTRATION OF SINGLE ISOLATED GUINEA PIG VENTRICULAR MYOCYTES. V.K. Sharma, M. Korth, D.J. Williford and S-S. Sheu, Dept. of Pharmacology, University of Rochester, Rochester, N.Y.

Recent observations indicate that stimulation of α_1-adrenergic and muscarinic (low affinity) receptors is associated with enhanced membrane phosphoinositide (PI) turnover. The present study investigates the effect of the α_1-adrenoceptor agonist, methoxamine, and muscarinic receptor agonist, carbachol, on intracellular Ca^{2+} concentration ($[Ca^{2+}]_i$) and contractile activity in guinea pig heart. Both methoxamine (30 µM) and carbachol (300 µM) produced a positive inotropic effect in guinea pig papillary muscles contracting isometrically at a frequency of 0.5 Hz. Application of methoxamine (30 µM) for 10 minutes to single isolated cardiac myocytes loaded with fura-2 did not produce any change in $[Ca^{2+}]_i$ as measured by quantitative fluorescence digital imaging microscopy. In contrast, exposure of single myocytes to carbachol (300 µM) produced a small, but significant increase in $[Ca^{2+}]_i$ (20 nM). These results suggest that different cellular mechanisms may be responsible for the positive inotropic effect induced by stimulation of α_1-adrenergic and muscarinic receptors, although both receptor types have been shown to stimulate PI hydrolysis.

W-AM-C4 SELECTIVE BLOCK OF NA+ and K+ CHANNELS IN FELINE VENTRICULAR MYOCYTES.
C.H. Follmer, G.C. Buzby, Jr., N.K. Jurkiewicz, R.P. Stein, and T.J. Colatsky, Wyeth Laboratories, Inc., Philadelphia, PA

Selective block of myocardial sodium and potassium channels is believed to form the basis for the antiarrhythmic activity of various pharmacologic agents. We examined the possible chemical basis for channel specificity by comparing the effects of two benzene sulfonamide analogues (below) on inward sodium (INa), delayed rectifier (IK) and background potassium (IK1) currents in single feline ventricular myocytes using whole cell voltage clamp techniques. With pulses from -120 to -30 mV (20°C), the 4-NH2 analogue (100μM) blocked INa by 64% at 1.0 Hz, while the 4-NO2 analogue (100μM) reduced INa by only 14%. Both analogues, however, completely blocked IK tails following 750 msec steps from -40 to +40 mV (35°C), and reduced IK1 by ~30% at -110 mV. The relative effects on INa were not predicted by considerations of molecular weight or lipid solubility. These data suggest that the aryl substituent plays an important role in determining the specificity of channel block, and that the presence of diffuse electronegativity in the hydrophobic region of the molecule can eliminate or reduce binding to the sodium channel blocking site.

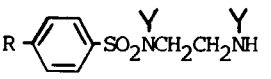

R	MW	log P	μ	σ
$-NH_2$	299	2.38	5.65	-0.66
$-NO_2$	329	2.65	8.08	+0.78

W-AM-C5 ESTIMATING CARDIAC TRANSMEMBRANE ACTIVATION AND RECOVERY TIMES FROM UNIPOLAR AND BIPOLAR EXTRACELLULAR ELECTROGRAMS: A SIMULATION STUDY
Bruce M. Steinhaus (Intro. by K.W. Spitzer), University of Utah, Salt Lake City, Utah 84112

A model of one dimensional action potential propagation was used to compare activation times (ATs) and recovery times (RTs) determined from unipolar electrograms (UEGs) and bipolar electrograms (BEGs) with the ATs and RTs determined from transmembrane action potentials (APs). Theory predicts that the time of the maximum negative slope of the UEG QRS complex corresponds to the time of maximum positive slope of AP depolarization. Similarily, the time of the maximum positive slope of the UEG T wave corresponds to the time of maximum negative slope of AP repolarization. The difference between the UEG AT and the AP AT (ΔAT) and the difference between the UEG RT and the AP RT (ΔRT) were small when the QRS complex and T wave were biphasic. This occurred during uniform propagation in a long, uniform, one dimensional cable. Nonideal conditions were studied as to their relative influence on ΔAT and ΔRT. Conditions which had the largest influence caused ΔAT to be up to 1.8 msec and ΔRT to be up to 30 msec (243 msec in certain conditions) and included: changes in activation sequence, propagation in a short cable, and propagation through regions of nonuniform coupling resistance or nonuniform membrane properties. Conditions which had a smaller influence on ΔAT and ΔRT included: variations in measuring distance from the simulated tissue surface, nonzero reference potentials and the addition of distant events. BEG ΔATs and ΔRTs were less than UEG ΔATs and ΔRTs when distant events significantly contributed to the UEG waveform, but under other conditions BEG and UEG ΔATs and ΔRTs were comparable. Results showed that ATs and especially RTs from electrograms can be markedly affected by conditions independent of changes in the underlying AP waveforms.

W-AM-C6 ACTIVATION OF A K^+ CURRENT BY EXOGENOUS G PROTEINS IN ATRIAL MYOCYTES.
G. Szabo, I.H. Pang†, and P.C. Sternweis†. Univ. of Texas Medical Branch, Galveston, Tx, 77550, and †Univ. of Texas Health Science Center, Dallas, Tx, 75235.

Isolated bullfrog atrial myocytes were voltage-clamped using a modified whole-cell patch clamp technique which allows rapid exchange of the solution in the patch pipette (J.Y. Lapointe and G. Szabo, Pflügers Arch, in press). With large pipettes (2-4 μM diameter) containing a standard internal solution (in mM: 80 K Aspartate, 30 KCl, 1 EGTA, 5 HEPES, pH 7.4) and 1-3 mM Mg ATP, the K currents of the cell, mainly I_{K1}, remained unaltered for up to 45 min. of recording. Perfusion of the patch pipette with internal solution containing 32 or 71 nM 41 kD α subunits (α_{41}) of a guanine nucleotide binding (G) protein purified from bovine brain and previously activated with guanosine-5'-(γ-thio)triphosphate (GTPγS) produced within 20 min. of perfusion stable ionic currents (∿ 40 pA at -5 mV) having inwardly rectifying IV characteristics similar to that produced by the muscarinic agonist acetylcholine ($I_{K(M)}$). Similar results were obtained with 5 nM activated α subunit (obtained from Dr. A.M. Brown, Baylor College of Medicine) of a red blood cell G protein. The α-subunit induced currents, however, were smaller than $I_{K(M)}$ (∿ 80 pA) and did not exhibit the characteristic voltage-dependent relaxation features associated with $I_{K(M)}$. Perfusion with the α_o (39 kD, 32 nM) subunit from brain had no effect. Non-activated, GDP-bound α_{41} (127 nM) produced much smaller (< 15 pA) increases in the K^+ current. We conclude that the activated α_{41} G protein subunit opens an inwardly rectifying K^+ channel in intact cardiac myocytes. Whether this current is identical to that produced by muscarinic agonists, remains to be established.
Supported by NIH grants HL37127 and GM31954.

W-AM-C7 DOUBLE BARREL K+ SELECTIVE MICROELECTRODE MEASUREMENTS IN SUBENDOCARDIAL PURKINJE FIBERS SURVIVING IN 3 HOUR INFARCTS. K.P. Dresdner, M.S. Hanna, R.P. Kline, and A.L. Wit, Pharmacology Dept., Columbia University, College of Physicians & Surgeons, New York, N.Y. 10032.

Using endocardial strips of canine left ventricle, we simultaneously measured intracellular K+ activity (aKi) and maximum diastolic potential (MDP) in subendocardial Purkinje fibers from infarcted hearts (IPF) surviving 3 hours after ligation of the anterior descending coronary artery. Mean (± S.D.) MDP and potassium equilibrium potential (EK; calculated from aKi) were averaged by hours of tissue bath superfusion, and compared to previous results from control fibers and IPF surviving at 24 hours post-ligation (See Dresdner et al., Circ.Res. 60(1):122-132, 1987). During the first hour of superfusion (see Table) mean EK reduction compared to control from normal hearts equalled 89 % of MDP depolarization for 3 hour IPF, but only 54 % for 24 hour IPF. Linear regressions on all data for up to 6 hours of superfusion (see Table) showed that IPF surviving 24 hours after ligation displayed slopes of MDP/EK > 2.0. IPF surviving 3 hours after ligation and controls showed slopes of MDP/EK < 0.5. Summary Table shows that between 3 and 24 hours after ligation marked changes in MDP dependence on EK occur; such that for similar EK reduction, MDP is more depolarized 24 hours after ligation than at 3 hours. This suggests a change in membrane conductance sometime 3 to 24 hours after the onset of myocardial infarction.

	MDP (mV)	EK (mV)		LINEAR REGRESSION (mV)	
Control PF	-85.0 ± 4.5	-97.2 ± 4.7	(n= 56)	MDP = 0.35 EK - 50	(n= 56 cells)
3 Hour IPF	-71.7 ± 9.0	-85.4 ± 5.6	(n= 17)	MDP = 0.42 EK - 37.6	(n= 49 cells)
24 Hour IPF	-50.1 ± 13.7	-81.2 ± 6.9	(n= 32)	MDP = 2.04 EK + 116.	(n= 160 cells)

W-AM-C8 **DETERMINANTS OF ACTION POTENTIAL DURATION IN A CONNECTED ARRAY OF MYOCYTES.** Kenneth R. Courtney, Bruce C. Hill, George T. Daughters and Neil B. Ingels. Research Institute, Palo Alto Medical Foundation, Palo Alto, CA.

In order to determine how the electrophysiology of an array of connected cells differs from that of a single cell, myocytes were modeled using the Beeler-Reuter equations for ionic currents. We found that the action potential duration (APD) of a single cell had the following important determinants: (1) a slow, plateau phase of repolarization attributable to both inactivation of slow inward current and activation of delayed potassium current and (2) a rapid, regenerative phase of repolarization caused by both rapid deactivation of slow inward current and inward rectification of potassium conductance.

When cells were coupled we found that (3) the presence of a neighboring cell that *does not fire* can reduce APD by up to 35%, due to its loading effects, while (4) a neighbor that *does fire* can prolong APD by about 15%. Finally, when an AP was propagated through a line of 5 cells they were activated with progressive delays (26 ms total delay), but repolarized much more synchronously (9 ms delay). This synchronization results from the better coupling of cells during their plateau phases, compared to coupling at rest, caused by the rectifying characteristics of potassium conductance. We conclude that a cell's APD is profoundly influenced by interactions with its neighboring cells, with K channel rectification playing a key role. Mechanism (3) above could be responsible, in part, for the shortened APDs observed in damaged myocardium.

W-AM-C9 A COMPUTER MODEL FOR ANALYSIS OF SYNCYTIAL EFFECTS OF LOCALIZED TRANSIENT INWARD CURRENTS IN VENTRICULAR MYOCARDIUM. Charles Nordin, Albert Einstein College of Medicine, Bronx, NY

We have used the results of voltage clamp experiments with isolated guinea pig myocytes to develop a computer model, based on electrical network theory, to describe the diastolic electrical behavior of heterogeneous regions of myocardial syncytia, and to analyze the response of such regions to localized transient inward currents (i_{ti}). The model incorporates measurements of i_{ti} and current-voltage relationships (CVR) we have obtained in both normal and depolarized (-20 to -30 mV) myocytes. Unlike conventional cable theory, the model treats the cell membrane as an active current generator, whose response varies as a function of voltage according to an experimentally measured diastolic CVR. Each cell is treated as a voltage node connected to other cells by gap junctions whose electrical resistance (r_j) is variable. The model demonstrates: 1) Localized i_{ti} (1-4 nA) cause depolarization of only a few millivolts in healthy, normally coupled myocardium. 2) In contrast, i_{ti} in a single cell within regions of 9-27 abnormal cells (depending on number of junctions) can cause voltage deflections sufficient to generate action potentials if r_j is 10-15 Mohms. If the number of junctions between abnormal cells is reduced to 2, as few as 3 cells can initiate action potentials from i_{ti}. 3) Unlike its effect on homogeneously distributed i_{ti}, the change in the CVR caused by low $[K+]_o$ enhances the generation of action potentials from localized i_{ti} only when r_j is increased and the number of junctions is decreased. 4) At the interface of larger blocks of normal and depolarized myocytes, no more than 4-10 layers of cells, all in the abnormal region, can initiate action potentials from i_{ti} as small as 2 nA. This semiempirical model thus confirms that surprisingly small regions of myocardium can generate abnormal rhythmic activity if uncoupling is present.

W-AM-C10 CCD VIDEO IMAGING OF CARDIAC ELECTRICAL ACTIVITY. G. Nassif*,F.Fillette & P. Aouate. Hopital Salpetriere, Paris, France (Intr. by L. Zablow).
* Now at Columbia Univ., Dept. of Pharmacology, NYC, NY 10032

The use of Charge Coupled Device (CCD) video cameras offers the possibility of making very high spatial resolution images of cardiac electrical activity.To test the feasibility of this approach we used a Sony XC37 camera (384 X 491 pixels, 30 frames/sec., 3 Lux sensitivity)to visualize surface fluorescence of sheep ventricular myocardium stained with the voltage sensitive dye WW781. Hearts were stained by incubation with Tyrode solution containing 0.4 g/l WW781. The fluorescence was imaged onto the CCD by a zoom-telelens (Soligor, f:3.5/70-220 mm) and a Schott RG665 long pass filter was used to reject the illumunation. Video signals were stored on a BVU tape recorder (Sony) using NTSC standard. The red (632.8 nm) light from a Helium-Neon laser was used to excite the fluorescence from the WW781 dye. Optical action potentials from discrete sites over an area of approximately 4 square centimeters were obtained by positioning 9 separate 5 mW HeNe lasers (NEC, Japan). Resting fluorescence from these sites appeared as spots of light in the video frame. During propagated activation caused by electrical stimulation we observed brightening of these spots, over 3 consecutive frames, due to action potential depolarization. We now believe that it is possible to image the fluorescence of a globally illuminated area. Such a technique would be of great use for the study of arrythmias on experimental models.

W-AM-C11 Na CURRENT (I_{Na}) AND INWARD RECTIFYING K CURRENT (I_{K1}) IN CARDIOCYTES FROM NORMAL AND HYPERTROPHIC RIGHT VENTRICLES OF CAT. PL Barrington, RD Harvey, DJ Mogul, AL Bassett and RE Ten Eick; Pharmacology, Northwestern University, Chicago, IL 60611.

Transmembrane action potentials (AP) recorded from cat papillary muscles (PM) that are obtained from hypertrophied right ventricles (HRV) are prolonged relative to those recorded from PM of normal right ventricles (NRV). Using the whole cell patch voltage clamp technique, I_{Na} and I_{K1} were elicited from myocytes from HRV and NRV to determine if any change(s) in the size or time course of these two components of the whole cell current could underlie the increased AP duration (APD) associated with RV hypertrophy. HRV was induced by subjecting cats to 2X normal pulmonary artery pulse pressures for 5-7 months. Hypertrophy was documented morphometrically using high power light micrographs. The peak amplitudes of both I_{Na} and I_{K1} were larger in cells from HRV than in cells from NRV, even when the currents were normalized to the cellular membrane capacitance to account for the fact that mean sarcolemmal area was 1.3X greater in HRV cells than it was in NRV cells. The time courses of both these 2 components of membrane current were qualitatively similar in NRV and HRV cells. However, relative to NRV, the time constant for slow inactivation of I_{Na} was decreased at membrane voltages positive to -10 mV. AP's simulated using the Di Francesco and Noble model for myocytes indicates that the change in PM APD associated with pressure overload-induced right ventricular hypertrophy cannot be explained by any differences from normal in the I_{Na} and/or I_{K1} observed in HRV cells. These findings imply that a change in some other component or components of the whole cell current must be involved. Alternatively, perhaps cells derived from RV free wall are not electrophysiologically analogous to cells composing papillary muscle.

W-AM-C12 INHIBITION OF Na,K-PUMP CURRENT IN GUINEA PIG VENTRICULAR MYOCYTES BY DIHYDROOUABAIN OCCURS AT BOTH HIGH AND LOW AFFINITY SITES.
David Mogul, Helge Rasmussen, Donald Singer, and Robert Ten Eick. (Intr. by A. Veis)
Depts. of Electr. Engrg., Medicine, & Pharmacol., Northwestern Univ., Chicago, IL

Binding of cardiac glycosides (CG) to the Na^+,K^+-dependent ATPase has been shown to occur at both high and low affinity sites. However, recent reports suggest that CG-induced inhibition of electrogenic Na,K-pump current (I_{pump}) occurs with simple first-order binding kinetics at relatively low affinity sites. This implies that high affinity binding sites have little to do with Na,K-pump inhibition during exposure to CG. Recently we reported data suggesting that both high and low affinity binding could be involved with CG-induced inhibition of I_{pump}. Because of the conflicting findings, we investigated the concentration dependence of I_{pump} inhibition by dihydroouabain (DHO) in guinea pig ventricular myocytes using wide-pore patch pipets to "fix" internal Na^+ activity at ~30 mM and to voltage clamp at -40 mV (T=34°C). Holding current (I_h) was monitored and the difference between steady state I_h before and after external exposure to 9 concentrations (range, 0.01-1000 μM) of DHO (I_{dif}) was measured and normalized to cellular membrane capacitance. The concentration dependence of the inhibition of I_{pump} was biphasic and well fitted to a 2 binding site model with inhibitory K_D's of 0.05 μM and 64.5 μM. This is consistent with previously reported ^{3}H-ouabain binding studies in guinea pig myocardium. These findings indicate that the electrogenic properties of the Na,K-pump can be inhibited by CG binding to both high and low affinity sites.

W-AM-D1 DOES THE EXTRACELLULAR MATRIX AFFECT ION FLUXES? EVIDENCE THAT INTERSTITIAL STRUCTURES IN SKELETAL MUSCLE BIND AND SLOW THE DIFFUSION OF SMALL IONS AND MOLECULES. J. Walter Woodbury, Dept. Physiology, School of Med. U. of Utah, Salt Lake City, UT 84108.

Excised frog sartorius muscles (ca. 30 mg) were soaked for about 2 hours in solutions containing radioactive Cl^-, I^-, benzoate$^-$ (Benz), trichloroacetate$^-$ (TCA), TEA^+, ^3H_2O or antipyrine and then washed out for 24 to 48 hours by collecting the superfusate in a series of vials for 2 to 20 min/vial. Efflux was normalized by dividing the net cpm in each vial by collection time, tracer soak concentration (cpm/mm^3) and muscle wet weight (units: % muscle volume cleared of tracer/min). Tracer concentration, [soak], was 0.1 to 10 mM. These experiments were done to study the effects of cell and bath pH on exotic anion fluxes and in most experiments Benz or TCA were used. The results were unexpected; measured anion effluxes were 10 to 1000 times larger than expected from the traditional, two comparment model of muscle washout. Plots of log (efflux) versus time often had no linear region attributable to the plasma membrane. The curves show a characteristic continual flattening. This flattening is visible in most published efflux curves regardless of the tissue or tracer used. Other experiments show that connective tissue (CT) is the major source of the excess efflux for $t > 300$ min and that CT efflux is accurately described by the diffusion equation with $D \sim 10^{-12}$ cm^2/s. For $t < 300$ min, there is a large unaccounted efflux remaining after CT and transmembrane effluxes are subtracted. This unaccounted flux is likely from a diffusion barrier (bulk structure) interposed between cells and bath because: (1) There is a large delay (~30 min, vs < 5 min expected) between a change in bathing solution and the resulting change in efflux. (2) Some efflux curves have a distinct inflection point. The [initial interstitial tracer]/[soak] ratio is calculated to be between 2 and 10. Tentative conclusion: Interstitial structures may alter transmembrane fluxes by binding ions and impeding their diffusion. These structures are apparently quite non-selective because similar results were obtained with all the small tracer molecules tested: anion, cation or neutral.

W-AM-D2 **Reciprocal Inhibition Between Identified *Aplysia* Neurons Maintained in Culture.** D. Kleinfeld, G. F. Raccuia & H. J. Chiel*, Dept. of Molecular Biophysics, AT&T Bell Laboratories, Murray Hill, NJ 07974 and *Dept. of Biology, Case Western Reserve University, Cleveland, OH 44106

Reciprocal, inhibitory synaptic connections are a feature of many small neural circuits. As a step toward understanding the role of such connections, we studied the formation of inhibitory synapses between neurons isolated from the abdominal ganglion of *Aplysia californica*[1]. Circuits containing two cells were constructed by co-culturing pairs of left upper quadrant (*LUQ*) neurons and *L*10 neurons. We observed an inhibitory connection from *L*10 to *LUQ* in all of the *LUQ*/*L*10 pairs (n=11), in agreement with Camardo *et al.*[2]. We further observed reciprocal inhibitory connections between neurons in 55% of these *LUQ*/*L*10 pairs (n=11) and 40% of *LUQ*/*LUQ* pairs (n=5; see Figure). None of the *L*10/*L*10 pairs formed reciprocal inhibitory connections (n=19). The connections in some pairs of neurons contained both electrical and chemical components; relatively fast electrical excitation ($\tau \sim 0.1$ s; $V_{post}/V_{pre} \sim 0.3$) was followed by slower, chemically mediated inhibition ($\tau \sim 1$ s to 10 s). These dual-action synapses may be useful for constructing neural circuits that produce rhythmic output[3,4].

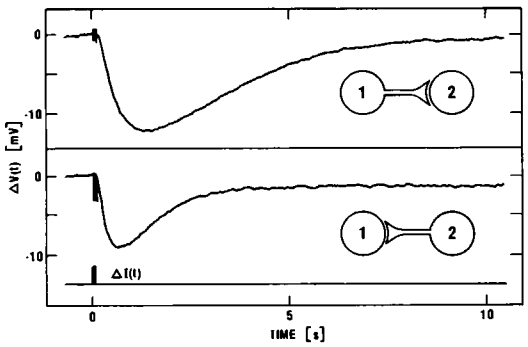

(1) Schacher & Proshansky 1983 *J. Neurosci.* 3:2403. (2) Camardo, Proshansky & Schacher 1983 *J. Neurosci.* 3:2614. (3) Sompolinsky & Kanter 1986 *Phys. Rev. Lett.* 57:2861. (4) Kleinfeld 1986 *PNAS* 83:9469.

W-AM-D3 TRANSDUCTION SENSITIVITY APPROACHING THE LIMIT GIVEN BY THE SPONTANEOUS BROWNIAN MOTION OF THE HAIR BUNDLE. W. Denk and W. W. Webb, Applied Physics, Cornell University, Ithaca, NY 14853.

We have measured simultaneously the spontaneous motion of the sensory hair bundles of the frog sacculus hair cells and the transmembrane potential fluctuations in the same cell. Position fluctuations were measured by remote optical sensing of hair bundle displacements by laser illuminated differential interference imaging microscopy (Denk and Webb, Bull. Am. Phys. Soc. 32, 645, 1987) and membrane potentials were recorded with high resistance internal micropipette electrodes. Cross correlation of these two signals showed that the transduction mechanism is indeed activated by the thermal motion of the hair bundle. In many cells the mechano-electrical transfer function (transduction spectrum) could be determined from this cross correlation. Tuning of the transduction coincided with a peak in the electrical noise spectrum. Transduction coefficients at the peak of the transduction tuning curves ranged from 10 mV/micron to 2000 mV/micron. The spontaneous motion spectra did not peak but began to roll off at frequencies above the transduction tuning peaks. At the peak frequency the intracellular electrical noise power density was usually about 5-10% correlated with the hair bundle motion; in some cells cross correlation values up to 40% could be observed. This result implies that the sensitivity of the hair cells at the optimum frequency approaches about 40% of the theoretical limit given by spontaneous mechanical fluctuations.

We wish to acknowledge the help of A. J. Hudspeth in the initial stages of this work and financial support by NIH (GM33028) and an IBM graduate fellowship for W.D.

W-AM-D4 DEPOLARIZATION RELEASE COUPLING IN THE *IN VITRO* CRAB T-FIBER SYNAPSE. J-W. Lin* and R. Llinás. Dept. Physiol. & Biophys., N.Y. Univ. Med. Ctr., 550 1st Ave., New York, NY 10016.

The crab T-fiber is one of the few synapses where chemical transmission may be studied intracellularly at pre- and postsynaptic sites simultaneously (Blight & Llinas: Phil. Trans. Roy. Soc. 290, 1980). To further characterize the properties of this junction, the preparation was simplified for direct *in vitro* study. The isolated preparation demonstrated functional properties similar to those previously reported *in situ*. The presynaptic current injection can be delivered very close to the release site (1 to 1.5 mm from the junction where λ is as long as 60 mm) and the voltage recording electrode can be positioned at the presynaptic release site. Under these conditions the properties of the postsynaptic potential (e.g. amplitude, latency, rate of rise, and waveform) were similar to those observed *in situ*. Furthermore, the presynaptic terminal could be depolarized sufficiently to attain the suppression potential, +30 to +50 mV, which was similar to that in squid giant synapse (Llinás et al., Biophys. J.: 33, 1981; Augustine et al.: J. Physiol. 367, 1985). A well defined "off" EPSP was observed at the end of the large presynaptic depolarization pulses. The depolarization release coupling exhibited a sigmoidal relationship with a peak value at -10 mV and E-fold increase in EPSP amplitude of 4.7 mV. Preliminary voltage clamp attempts indicated that the presynaptic terminal may be depolarized with a 10-90% rise time of 100 µsec. This synapse represents another preparation in which calcium entry and not presynaptic voltage is the triggering signal for transmitter release. In addition, this synapse has the advantage of being a tonically releasing junction as opposed to the squid giant synapse which is a more phasic transmitting system. (Supported by NS07942 and NS14014)

W-AM-D5 PROPERTIES OF A Ca-BINDING SITE ON NEUROFILAMENT PROTEINS. Ronald F. Abercrombie and Jeffrey P. Jackson, Department of Physiology, Emory University School of Medicine, Atlanta, GA 30322.

We have made two types of measurements suggesting that neurofilaments obtained from Myxicola giant axons tightly bind stoichiometric amounts of calcium. (a) Using the autoradiographic method of Maruyama et al. (J. Biochem. 95:511, 1984), axoplasmic proteins were resolved by sodium dodecylsulfate, transferred to nitrocellulose membranes, placed in solutions containing µM Ca with tracer ^{45}Ca, rinsed, and overlaid with X-ray film at -150°C. This revealed that the 150,000-160,000 molecular-weight neurofilament proteins are the most prominent Ca-binding proteins of axoplasm. (b) By a process of freezing, thawing, and centrifuging, the axoplasmic proteins can be divided into two fractions: a pellet fraction that is enriched (≈80%) with neurofilaments, and a supernatant fraction depleted (≈20%) of neurofilaments. The Ca-binding properties of these two fractions differed in several respects as determined by equilibrium dialysis at pH 6.8. The supernatant fraction had a lower specific, and a higher nonspecific, binding component than the pellet fraction. The nonspecific component became larger in solutions of elevated pH. The specific Ca-binding component of the pellet fraction had a K_1 of ≈1 µM and a capacity of ≈4 µmoles Ca/g protein. Elevating the pH from 6.8 to 7.5 reduced the capacity of Ca binding to the pellet fraction but had minimal effect on the Ca affinity. The capacity measured at pH 6.8 corresponds to ≈1 Ca bound per 150,000 molecular-weight neurofilament monomer unit. Based on the molar concentration of neurofilament protein in axoplasm, these sites could hold ≈100 µM Ca per kg of Myxicola axoplasm. Supported by NIH NS19194.

W-AM-D6 BIOMAGNETIC STUDIES OF EPILEPTIFORM FOCI WITH SQUID

J.Vartzopulos,P.Anninos,Dept. of Medicine,Neurology clinic,Alexandroupolis , Greece.

Our work is based on studies of epileptic patients using the biomagnetometer SQUID,which due to its better spatial resolution can localize the epileptiform focus by measuring separately the intensity of magnetic field emitted from circular areas of the cortex (in our case the circle has an effective diameter of 2,36 cm,i.e. the diameter of the SQUID's coil).We expressed our results in terms of iso-spectral Amplitude (ISO-SA) distribution for each spectral component or frequency bands,so that we get what we called ISO-SA maps.We examined 3 groups of epileptic patients under anticonvulsant drug therapy.Each patient we measured 5 times with one month interval between the examined times.The patients in the first group are characterized by a complete absence of epileptic attacks in the 4month period and also 2 months before and after the examined time.The patients in the second group were examined 10 days after an epileptic attack but they did not have any attack thereafter.Finally in the third group are patients with frequent epileptic attacks in the above mentioned time span (4 months).From our preliminary results we found that we have definite variations in the spatial ISO-SA map distribution which are dependent on whether or not we have epileptic attacks.Thus in the first group the spatial ISO-SA map distributions in the 2-7 Hz band seems that decreases whereas in the second group it decreases as we move further away from the epileptic attacks and finally the third group exhibits more or less constant spatial ISO-SA map distributions.From the above results we can see for the first time a) the effect of the anticonvulsant drug treatment and b) that it is possible to predict the probability of an attack,so that to modify the pharmacological treatment.

W-AM-D7 A DISYSTEM MODEL OF NATURAL INTELLIGENCE. Michael Parks & Charles Walter

A model of intelligent behavior based on the macro-architecture of brain function is discussed. The disystem model is based on neurophysiological evidence of contralateral symmetry in brain morphology and coherence of brain activity. Experimental evidence based on positron emission tomography (PET) technology leads to two viewpoints regarding the symmetry of metabolic activity in contralateral brain hemispheres. One viewpoint, based on statistical means taken from the two hemispheres, suggests left/right asymmetries in certain situations. The other viewpoint, based on observed correlations between the spatial organization of glucose metabolism in the two hemispheres, an independent statistical criterion, suggests a co-operative model. The PET data reported here is used in computer simulations to illustrate these two points of view. A conjecture that maintenance of the observed property of contralateral symmetry is an important feature of the micro-architecture of intelligent behavior is discussed.

W-AM-D8 VOLTAGE SENSITIVITY OF THE ADAPTATION RATE IN ISOLATED VERTEBRATE HAIR CELLS.

J. A. Assad and D. P. Corey, Neuroscience Group, Howard Hughes Medical Institute, Dept. of Neurology, Massachusetts General Hospital, and Dept. of Neurobiology, Harvard Medical School, Boston, MA

The receptor current of bullfrog saccular hair cells shows a pronounced adaptation in response to maintained mechanical stimuli. This involves a relaxation in the apparent stimulus reaching the mechanically sensitive transduction channels and is characterized as a shift of the current-displacement [I(X)] curve along the X axis (Eatock et al., 1987). While the phenomenon is known to be calcium-dependent, its cellular basis is poorly understood, in part because early studies did not allow for control of the intracellular ionic environment. Recent whole-cell patch clamp measurements have afforded such control but have not revealed adaptation (Ohmori, 1985; Holton and Hudspeth, 1986). We have developed a preparation of isolated hair cells from the bullfrog sacculus; they are mechanically sensitive and exhibit adaptation. Single cells were plated onto concanavalin-A-coated coverslips. Pipettes were sealed to the basolateral surface. The bath contained normal frog Ringer with 4 mM Ca^{++}; pipettes contained 120 mM Cs^{+}, 2 Mg^{++}, 85 aspartate or 43 Cl^{-} and 43 F^{-}, 10 EGTA and 5 HEPES.

Step displacements of the stereociliary bundle towards the kinocilium for 100 ms elicited a transduction current that decayed to a steady level 1/2 to 1/3 of the peak magnitude. The decline was a result of transduction channels closing: membrane conductance declined with the same timecourse. Channels closed because the I(X) curve shifted: the curve was measured directly with test steps during the adapting step. A high-resolution video monitor showed no motion of the cell body or slippage of the stimulus probe.

A striking feature of the adaptation was a strong voltage dependence: the timecourse at negative potentials was comparable to that measured with microphonic recording, but the shift was virtually absent at positive potentials. Voltage dependence could be an intrinsic property of the adaptation, suggesting a transmembrane element. More likely, it reflects the voltage dependence of calcium entry through transduction channels. If so, the site of calcium's action must be intracellular. The voltage effect on the timecourse occurs within 10 msec, which is less than the predicted diffusion time of calcium to the soma, so the site may be near the tips of the stereocilia.

W-AM-D9 **INHIBITORS OF PROTEIN KINASE C (PKC) BLOCK LONG-TERM POTENTIATION (LTP) IN RAT HIPPOCAMPAL SLICES.** *Roberto Malinow, Daniel V. Madison and Richard W. Tsien.*

Department of Cellular and Molecular Physiology, Yale School of Medicine, New Haven, CT. 06510.

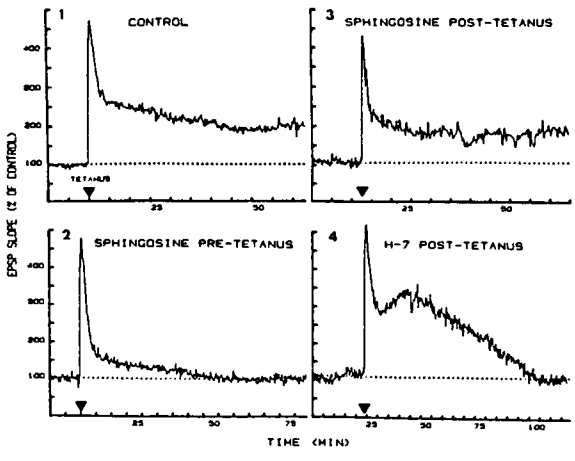

Activation of PKC by phorbol esters (Malenka et. al. 1986) or direct injection of PKC (Hu et. al. 1987), potentiates hippocampal synaptic transmission, suggesting that PKC may participate in the induction of LTP. Using PKC blockers, we have tested if tetanus-induced LTP requires PKC activation and whether the continuous activity of this kinase is required to maintain LTP.

We are studying LTP of synaptic transmission in the Schaffer collateral-CA1 pathway in slices of rat hippocampus (fig. 1). Sphingosine (10 μM), which inhibits PKC activity at its regulatory domain (Hannun et. al. 1986), blocks LTP when applied before (fig. 2) but not immediately after (fig. 3) tetanic stimulation. H-7 (300 μM), which inhibits protein kinases at the ATP-binding catalytic domain, blocks LTP when applied before as well as after the tetanic stimulation (fig. 4). Thus, PKC activation may be necessary to induce LTP, and continued H-7-sensitive activity may be required to maintain LTP.

W-AM-D10 EFFECTS OF NGF ON CA CHANNEL DISTRIBUTION IN PC-12 CELLS. D.D. Friel and R.W. Tsien. Dept. of Cellular and Molecular Physiology, Yale Medical School, New Haven, CT 06510.

Nerve growth factor (NGF) causes PC-12 cells to assume a variety of neuronal characteristics. Accompanying the induction of neurite outgrowth by NGF is a dramatic loss in the dihydropyridine sensitivity of K^+-stimulated ^{3}H-norepinephrine (NE) release. It has been suggested that this loss in sensitivity results from a change in the types of Ca channels which control NE release. We have studied the effects of NGF on Ca channel expression in PC-12 cells by comparing single channel currents through cell-attached patches from cells before and after (2-21 d) treatment with NGF. Bathing solutions contained high-K^+, and pipettes contained 110 mM Ba, 1 μM TTX and 2 μM Bay K 8644. Unitary currents resembling L- and T-type Ca channel currents were seen both before and after treatment with NGF, often in the same patch. The larger current (γ ~23 pS), seen in all undifferentiated cells and the soma and growth cones of most differentiated cells, displayed a slowly inactivating average current (A) and could be elicited from either V_H=-80 or -40 mV. In some patches from growth cones, only the smaller, T-like unitary current was observed; this current yielded an inactivating average current (nulls excluded) (B) and was not elicited from V_H=-40 mV. The sensitivity of the two unitary currents to dihydropyridines is under investigation.

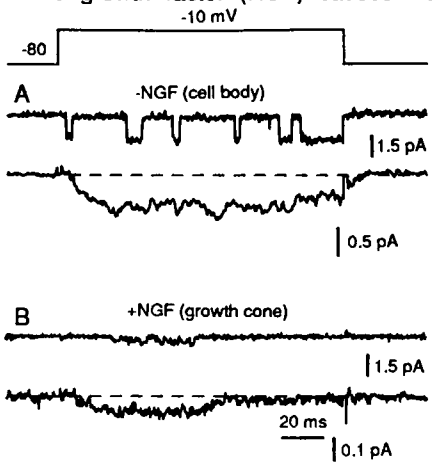

W-AM-D11 DEVELOPMENTAL CHANGES IN WHOLE CELL Na^+ AND K^+ CURRENTS FROM IDENTIFIED CHICK MOTONEURONS. P.M.Best*, D.P.McCobb#, & K.G.Beam#. Depts. of Physiology, *Univ. of Illinois, Urbana, IL 61801, and #Colorado State University, Fort Collins, CO 80523.

Because electrical activity is known to play an important role in neuromuscular development, we have begun to characterize ionic currents in embryonic chick motoneurons. We report on changes in ionic currents which have taken place between embryonic days 6 and 11, during which approximately half the motoneurons die. To identify them, motoneurons were retrogradely labelled by injecting limb buds of embryos with a lipophilic dye (di-I) 12-18 hours prior to dissociation of the cord. Whole cell currents were recorded with patch pipettes from labelled cells 3 to 24 hours after dissociation. The normalized Na^+ current density (pA/pF) increased from 72.3 ± 9.6 (mean ± S.E.M.) in motoneurons isolated from 6-day embryos to 124 ± 31.6 in those from 11-day embryos. Motoneuron Na^+ currents in both 6 and 11-day embryos were highly sensitive to TTX, with exposure to 100 nM drug causing ≥95% block. At least two K^+ currents were present in 6 and 11-day motoneurons. One was a non-inactivating, TEA^+ sensitive current whose normalized conductance (nS/pF) decreased from 0.82 ± 0.17 in 6-day motoneurons to 0.47 ± 0.08 in 11-day motoneurons. The second was an inactivating, 4-aminopyridine sensitive current (A current), whose normalized conductance was 0.46 ± 0.13 at day 6 and 0.59 ± 0.10 at day 11. Therefore, the ratio of A current conductance to total cell K^+ conductance increased from day 6 to day 11. These results indicate that motoneurons are undergoing maturational changes in electrical properties at the same time as other important developmental events are occurring. Supported by NIH grants NS24444 (KGB) and AR32062 (PMB).

W-AM-D12 MOBILIZATION, INFLUX AND BUFFERING OF Ca^{2+} IN NEURONS S.A. Thayer and R.J. Miller (Intr. by M. Villereal) Dept. of Pharmacological and Physiological Sci., University of Chicago, Chicago, IL 60637

$[Ca^{2+}]_i$ was measured in single central (hippocampus and striatum) and peripheral (sympathetic and sensory) neurons with fura-2 based microfluorimetry. Caffeine (10 mM) in Ca^{2+}-free medium, produced significant increases in $[Ca^{2+}]_i$ in the cell bodies of peripheral neurons with less frequent and smaller effects seen in central neurons. The caffeine-induced rise in $[Ca^{2+}]_i$ in peripheral neurons could be inhibited by the alkaloid ryanodine (1 μM) in a use-dependent manner. Dantrolene (10 μM) also inhibited the caffeine response but its effects were not use-dependent. Caffeine was generally ineffective in elevating $[Ca^{2+}]_i$ in the processes of these neurons. The peptide bradykinin (BK) also produced increases in $[Ca^{2+}]_i$ in sensory neurons in Ca^{2+} free media. BK released Ca^{2+} from intracellular stores presumably by its stimulation of IP_3 synthesis. The IP_3 sensitive stores appear to be distinct from those mobilized by caffeine. Indeed, these stores were consistently found in the processes of sensory neurons. Depletion of either intracellular store of Ca^{2+} produced a large increase in the ability of sensory neurons to buffer a Ca^{2+} load. Three Ca^{2+} channel types are present in these cells. Thus, when Ca^{2+} currents and $[Ca^{2+}]_i$ transients were measured simultaneously with whole cell patch-clamp and microfluorimetry the $[Ca^{2+}]_i$ transient depended on the population of channels activated. The transient that resulted from activation all three Ca^{2+} channel types (see fig.) was much larger than the transient resulting from activation of only the high threshold L type channel.

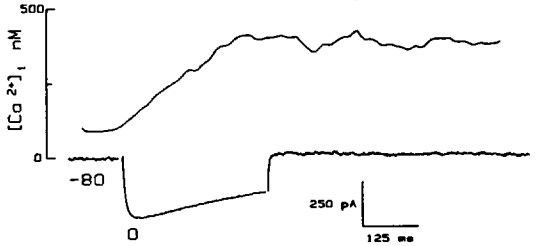

W-AM-D13 KINETICS OF CALCIUM CHANNEL BLOCKAGE BY CADMIUM IN CHICK SENSORY NEURONS. D.Swandulla and C.M.Armstrong, Dept of Physiology, Univ. of Pennsylvania, Philadelphia, PA, 19104.

Cd^{2+} block of whole cell Ca and Ba currents through fast deactivating Ca channels was studied in chick DRG cells. External Cd^{2+} (20 μM) almost completely blocked Ba pulse currents. Neither the I-V relation nor the activation kinetics, as determined by tail current measurements, were significantly affected by adding Cd^{2+} to the external solution. Cd^{2+} was ~2.5X more effective in blocking Ba current than Ca current. In contrast to the strong reduction of pulse current, Ca tail current was reduced by only ~40% with 20 μM Cd^{2+} at -80 mV. Tails exhibited 'hooks' as Cd^{2+} left the channels, particularly obvious near -40 mV (see figure, showing tails at -80,-60,-40 and-30 mV). Cd^{2+} reequilibration with the channels was almost complete after ~15 ms at -80 mV, and was much slower at more negative potentials (~55 ms at -130 mV). At +20 mV reequilibration was much faster, having a time constant of ~1.5 ms.

Supported by USPHS 12547 and by a grant of the Max Kade Foundation to D.S.

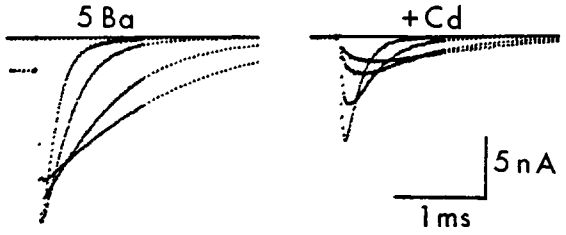

W-AM-E1 CALMODULIN SUPPORTS THE FORCE GENERATING FUNCTION IN TnC-DENUDED FIBERS: COMPETITION WITH PARVALBUMIN

J. Gulati, G. Orr*, and A. Babu
Depts of Medicine and *Mol Pharm, Albert Einstein College, Bronx, NY (Intro: T. Robinson)

The helix-loop-helix units comprising the four Ca^{2+} binding domains (A/B,C/D,E/F,G/H) of calmodulin and troponin-C are analogous, except that the affinity of E/F,G/H domains is modified. Also, there are conflicting reports on the ability of CaM to regulate the contractile function of muscle. CaM can regulate the ATPase activity of the isolated actomyosin as well as of myofibrils, but was found unable to replace the function of TnC in partially denuded fibers. In examining the issue here we make use of the fact that E/F,G/H domains in TnC are the Ca/Mg sites, but in CaM they remain Ca^{2+} binding domains. Skinned psoas fibers from rabbits were treated for TnC-extraction (Babu et al, JBC, 262:5815, 1987) to delete 70-75% of the TnC. These TnC-denuded fibers were permanently restored with purified TnC and EGTA, in composition (by SDS-PAGE) and in function (by Ca^{2+}-activation). In contrast, CaM with EGTA was completely ineffective, suggesting that the modification of the Ca/Mg sites was critical. However, with CaM in the presence of Ca^{2+}, the regulation was restored within 10-30 min. Returning to Ca-free solution immediately relaxed the fiber by releasing the CaM. These results demonstrate the ability of CaM to replace TnC and show that Ca^{2+} is required to override the site modification. Additional experiments were made of competition of CaM with CTnC and parvalbumin. They provide direct evidence that CaM reversibly adsorbs the denuded sites, and show that while the presence of E/F, G/H domains in CaM is essential for the occupation of the TnC-sites in the fiber, minor differences in the supersecondary structural orientations may be critical also.

W-AM-E2 CLONING, SEQUENSING AND EXPRESSION OF A FULL LENGTH RABBIT SKELETAL TROPONIN-C cDNA.

Q. Chen, J. Taljanidisz, S. Sarkar, T. Tao and J. Gergely. Dept. of Muscle Research, Boston Biomed. Research Inst.; Dept. of Neurology; and Dept. of Biol. Chem. & Mol. Pharmacol., Harvard Medical School; and Dept. of Anatomy and Cellular Biology, Tufts University School of Medicine, Boston, Massachusetts.

In order to gain a better understanding of how skeletal muscle contraction is regulated by Ca^{2+}, we have begun to use recombinant DNA techniques with a view to introducing specific amino acid changes at selected sites in troponin-C (TnC), and to studying the effects of these changes on its structure and function. To this end, we have isolated and characterized a full length cDNA coding for rabbit fast skeletal TnC. The complete nucleotide sequence of this cDNA contains the entire coding region, with 5' and 3' untranslated regions of 68 and 105 nucleotides, respectively. In agreement with Zot et al. (J.B.C., in press), we find that the derived amino acid sequence is identical to the published protein sequence (Collins et al., J.B.C. 252, 6356, 1977), except that the first two residues are reversed. The cloned gene was expressed in an E. Coli host using an expression vector that contains the T7 RNA polymerase/promoter system (Tabor & Richardson, PNAS, 82, 1074, 1985) in a medium containing ^{35}S-Met. The autoradiogram of the bacterial lysate shows a single major band whose mobility in SDS-PAGE is identical to that of purified rabbit skeletal TnC. The expressed protein was partially purified by ammonium sulfate and isoelectric (pH 4.1) precipitation and when subjected to electrophoresis in urea-EDTA gel, its mobility was again found to be identical to that of purified TnC. Finally, Western blot analysis showed that the band corresponding to the expressed protein reacts with goat anti-rabbit skeletal TnC. Thus the expressed protein appears to be identical to rabbit skeletal TnC.
(Supported by grants from N.I.H., AR-21673 and HL-05949, and MDA)

W-AM-E3 BIOLOGICALLY ACTIVE FLUORESCENT DERIVATIVES OF SPINACH CALMODULIN WHICH REPORT CALMODULIN TARGET PROTEIN BINDING.

J. David Johnson, John S. Mills, Michael P. Walsh and Karen Nemcek. Dept. of Physiological Chemistry, The Ohio State Univ. Medical Center, Columbus, Ohio (JSM, KN, and JDJ) and The Dept. of Medical Biochemistry, Univ. of Calgary, Calgary Alberta, Canada (MPW).

Spinach CaM has been labeled at cysteine 26 with the sulhydryl selective probe 2-4' maleimidyl-anilinonaphthalene-6-sulfonic acid (MIANS) to produce MIANS-CaM. The inteaction of MIANS-CaM with CaM-binding proteins was studied by fluorescence enhancement accompanying the protein-protein interactions. MIANS-CaM bound to smooth muscle myosin light chain kinase with a Kd of 9nM causing a 4.6-fold fluorescence enhancement. Caldesmon bound with a Kd of 250 nM causing a 2-fold fluorescence enhancement. Calcineurin (CaN) bound to MIANS CaM with a Kd < 5 nM causing an 80% increase in fluorescence. On the other hand, binding of the CaM antagonist drugs prenylamine and calmidazolium or the potent peptide antagonist melittin did not alter MIANS fluorescence. MIANS-CaM activated brain cGMP Phosphodiesterase and CaN as effectively as unlabeled CaM. Spinach CaM was also labeled with three other sulfhydryl reagents, 6-acryloyl 2-dimethylaminonaphthalene, 2,5 dimethoxy stilbene-4 maleimide and rhodamine X maleimide. CaN bound to the highly flurescent rhodamine X maleimidyl CaM with a Kd of 1.4 nM causing a 25% increase in polarization. Both MIANS-CaM and rhodamine X CaM were used to monitor the Ca^{++} dependence of the interaction between CaM and CaN. Half maximal binding occurred at pCa = 6.7 to 6.8 in the absence of Mg^{++}, or at pCa = 6.3 in the presence of 3 mM Mg^{++}. In both cases the dependence of the interaction was cooperative with respect to Ca^{++} (Hill coefficients of 1.7 to 2.0). Use of these fluorescent CaMs should allow accurate monitoring of CaM interactions with its target proteins and perhaps their localization within the cell. Supported by NIH (AM33727,HL01449), the MDA & the Med Res Counc of Canada MT-9097.

W-AM-E4 STRUCTURE/FUNCTION RELATIONSHIP OF THE LC2 LIGHT CHAIN OF SKELETAL MYOSIN INHIBITION OF PHOSPHORYLATION. Suzanne M. Pemrick and Edward Harper. Dept. of Biochemistry and Biophysics Prog. SUNY, Health Sci. Ctr. at Brooklyn, NY

LC2 alters filament assembly (Chowrashi et al (1988) in press); and Pi liberation as LC2-ATPfree for the actomyosin MgATPase (Pemrick (1988) in press). These effects involved 50% of bound LC2. Similarly, time course profiles of % LC2-P showed 50% of LC2 could be resistant to phosphorylation: 1 mg/ml = 10% inhibition (I); by 10 mg/ml, maximal or 50% I. The substrate profile of I was similar for HMM, negligible for S-1, and greatly enhanced for free LC2. LC2-P was not the inhibitor since inhibition was present at early times irrespective of the kinase concentration; LC2-P increased the initial rate, but had no effect upon the final % LC2-P. Inhibition was reversed completely by dilution to 1.0 mg/ml and was insensitive to additional kinase. Ionic strength had no effect upon I above 6.0 mg/ml or below 50% LC2-P. Otherwise, I was enhanced 10% between 0.05 to 0.1 M and solubility of myosin filaments occurred between 0.15 and 0.3 M ionic strength. The pattern of substrate inhibition was similar for LC2-deficient myosin -1 mol LC2/mol -except the initial rate of phosphorylation was decreased. Therefore, with respect to LC2-P formation, there are 2 populations of bound LC2. It is hypothesized that substrate inhibition is due to specific, concentration dependent, intermolecular associations of myosin requiring the two-headed, but not the filamentous structure of myosin. (Supported by USPHS grant HL22401 to SP)

W-AM-E5 FLUORESCENCE ENERGY TRANSFER BETWEEN CALDESMON AND CALMODULIN. C.-L. Albert Wang, Dept. of Muscle Research, Boston Biomedical Res. Inst., Boston, MA 02114

The smooth muscle thin filament protein caldesmon (CaD) binds to F-actin; the interaction is weakened upon addition of calmodulin (CaM) in the presence of calcium. Such interactions have been thought to be relevant to the regulation of smooth muscle contraction. We have carried out distance measurements in complexes involving CaD by fluorescence energy transfer. 1,5-IAEDANS attached to thiols of CaD was used as the donor, and 4-dimethylaminophenylazophenyl-4'-maleimide (DAB-Mal) attached to thiols of various protein components (CaM, TnC, and F-actin) as the acceptor. When the binary complex was formed between AEDANS-CaD and wheat germ CaM labeled with DAB-Mal at Cys-27 a small energy transfer was observed in the presence of calcium, but not in the absence of calcium. The transfer efficiency corresponds to a separation distance of 6.3 nm between the two probes in the presence of calcium (R_o for AEDANS and DAB taken as 4 nm). When CaM was replaced with DAB-TnC, a similar energy transfer efficiency was obtained as in the case of CaD-CaM, suggesting that the two homologous calcium-binding proteins bind to CaD at similar sites. The energy transfer, however, is not calcium-dependent; this is consistent with the steady-state titration, viz. TnC interacts with CaD both in the presence and in the absence of calcium. In the system containing AEDANS-CaD and F-actin with DAB-Mal attached to Cys-374, there was some energy transfer between CaD and F-actin, the distance (5.8 nm) being slightly shorter than those between CaD and CaM or TnC. These results may be interpreted as the actin-binding site being in the vicinity of the CaM- (and TnC-) binding site on the CaD molecule. The energy transfer disappeared when Ca/CaM was added, indicating that F-actin is dissociated from CaD by CaM in the presence of calcium. Supported by grants from NIH (AR32727 and BRSG RR05711).

W-AM-E6 POTENTIAL NONPRODUCTIVE INTERACTION OF MYOSIN SUBFRAGMENTS WITH ACTIN MEDIATED BY CALDESMON, M.E. Hemric, C.E. Benson, J.M. Chalovich; East Carolina University Medical School; Greenville, NC 27858

Smooth muscle caldesmon inhibits the actin-activated ATPase activity of both smooth and skeletal myosin subfragments (HMM and S-1) with similar caldesmon concentration dependencies. To determine the mechanism of this inhibition we have studied the binding of caldesmon and various myosin subfragments to actin in the presence of different nucleotides. Caldesmon competes with both smooth and skeletal HMM's and S-1's for binding to actin in pyrophosphate, AMP-PNP, and in rigor. With smooth HMM, smooth S-1, and skeletal HMM, a weak complex with actin-tropomyosin-caldesmon (A-T-C) may form although the binding of any myosin subfragment to A-T-C tends to displace the bound caldesmon. In contrast, the effect of caldesmon on the interaction of myosin subfragments with actin-tropomyosin, during steady-state ATP hydrolysis is dependent on the type of myosin subfragment. The binding of skeletal S-1 to actin-tropomyosin is greatly weakened by caldesmon whereas, in agreement with Lash et al. (1986 J. Biol. Chem. p 16155) the binding of smooth HMM is enhanced by caldesmon. Smooth S-1 and skeletal HMM also exhibit increased binding to actin in the presence of caldesmon, during ATP hydrolysis, but there is no clear relationship of this binding with inhibition of ATPase activity. On the basis of these experiments, and the interaction of smooth HMM and S-1 and skeletal HMM with a caldesmon affinity column, we propose that caldesmon functions by inhibiting the binding of myosin to the productive site on actin. A nonproductive interaction of myosin with A-T-C may occur. This interaction is unrelated to the inhibition of ATP hydrolysis although it could be important in the function of smooth muscle.

W-AM-E7 CALDESMON KINASE: KINETIC AND REGULATORY PROPERTIES AND PHOSPHORYLATION OF SYNAPSIN I. Gisele C. Scott-Woo and Michael P. Walsh, Dept. of Medical Biochemistry, University of Calgary, Alberta, Canada T2N 4N1.

Caldesmon (CaD), an actin- and calmodulin (CaM)-binding protein, has been implicated in the regulation of smooth muscle contraction. CaD is phosphorylated by endogenous protein kinase activity and phosphorylation blocks its ability to inhibit the actin-activated Mg^{2+}-ATPase activity of smooth muscle myosin. Several lines of evidence suggest that CaD itself is a kinase and this activity is an intermolecular autophosphorylation. CaD kinase activity is dependent on Ca^{2+} and CaM, with half-maximal activation at 0.06 μM Ca^{2+} and 0.14 μM CaM and maximal activation at 0.14 μM Ca^{2+} and 1 μM CaM. Activation decreases at higher concentrations of Ca^{2+} or CaM. The K_m (ATP) is 15.6 ± 4.1 μM (n=4). Of several potential substrates examined, only synapsin I is as good a substrate as CaD itself. Synapsin I phosphorylation (~2.0 mol P_i/mol synapsin I) is Ca^{2+}/CaM-dependent. CaD kinase phosphorylates the same site on synapsin I as does cAMP-dependent protein kinase, plus an additional site. Pre-phosphorylation of CaD results in loss of the Ca^{2+}/CaM-dependence of synapsin I phosphorylation. Synapsin I phosphorylation by CaD kinase occurs with half-maximal activation at 0.13 μM Ca^{2+} and maximal activation at 0.4 μM Ca^{2+}. Unlike autophosphorylation, only a small loss of activity occurs at higher [Ca^{2+}]. The K_m of CaD kinase for synapsin I is 88.5 nM. By a number of criteria, we show that CaD kinase is a distinct enzyme from other known Ca^{2+}/CaM-dependent protein kinases. In addition to its potential role in the regulation of smooth muscle contraction, CaD kinase may be involved in regulating neurotransmitter release through phosphorylation of synapsin I.

W-AM-E8 REGULATION OF SMOOTH MUSCLE PROTEIN KINASE C. Michael. P. Walsh and Gwyneth de Vries, Dept. of Medical Biochemistry, University of Calgary, Alberta, Canada T2N 4N1.

Protein kinase C (PKC) was partially purified from chicken gizzard smooth muscle by Ca^{2+}-dependent hydrophobic-interaction chromatography and ion exchange chromatography. This preparation was stable and could be stored for several months at -80°C in 10° (v/v) glycerol/0.05% (w/v) Triton X-100 without loss of activity. Further purification, however, resulted in rapid loss of enzymatic activity. Fast-performance liquid chromatography (gel filtration) revealed a Stokes radius of 33.7 Å, corresponding to a globular protein of M_r 61,500. Sodium dodecyl sulfate-polyacrylamide gel electrophoresis indicated a M_r of 80,000. The native enzyme is, therefore, monomeric. PKC activity was routinely assayed by the mixed-micelle assay of Bell *et al* [Methods Enzymol. 124, 353 (1986)] using histone III-S as the substrate, but at a Triton X-100 concentration of 0.03% (w/v) which was found to be optimal. PKC activity required Ca^{2+}, phospholipid and diacylglycerol (DG) for activity, with half-maximal activation at 4.62 ± 0.31 x 10^{-7} M Ca^{2+} (n=3) in the presence of saturating concentrations of L-α-phosphatidyl-L-serine and 1,2-diolein. No activation by Ca^{2+} was observed in the absence of DG. PKC required free Mg^{2+}, in addition to the $MgATP^{2-}$ substrate, for activity. The K_m for ATP was 19.9 ± 4.6 μM (n=4). Activity was highly sensitive to ionic strength, with half-maximal inhibition at 70 mM NaCl. Phosphorylation of the physiological substrates, platelet P47 and smooth muscle vinculin, was more strongly dependent on Ca^{2+} and lipids than was histone phosphorylation. Partial digestion with trypsin yielded a constitutively active fragment, as has been shown with other PKC's. A heat-stable protein inhibitor of PKC was also identified in smooth muscle. This inhibitor is immunologically non-crossreactive with the bovine brain 17 kDa heat-stable PKC inhibitor we have described previously [McDonald *et al* Biochem. J. 242, 695 (1987)].

W-AM-E9 COMPARISON OF THE EFFECTS OF INTACT TROPOMYOSIN AND NONPOLYMERISABLE TROPOMYOSIN ON THE ACTOMYOSIN S1 Mg ATPase ACTIVITY. D.H. Heeley, E. Lohmeier-Vogel and L.B. Smillie. MRC Group in Protein Structure and Function, Dept. of Biochemistry, University of Alberta, Edmonton.

We have investigated the role of the overlap region of tropomyosin (TM) in the regulatory properties of striated muscle thin filaments by using a truncated derivative of TM in a reconstituted actomyosin S-1 ATPase assay. The shortened form of TM (NPTM), generated by carboxypeptidase-A treatment and thereby eliminating its polymerisation and F-actin binding properties, has in a previous study carried out at an ionic strength of 75 mM, been shown to bind to F-actin (±Ca^{2+}) in the presence of troponin (Tn) (Heeley *et al*. (1987) J.B.C. 262: 9971-9978). At an S-1:F-actin ratio of 2:1 (ionic strength, 54 mM; F-actin, 4 μM; Tn, 1.14 μM) comparable levels of inhibition were observed for mixtures of NPTM + Tn (-Ca^{2+}) and TM + Tn (-Ca^{2+}). In both cases, maximal inhibition was attained at a TM(or NPTM):F-actin ratio of approximately 0.15. Large differences were noted, however, in the release of inhibition by Ca^{2+}. S-1 titrations showed that when NPTM was substituted for TM, in the presence of Tn (+Ca^{2+}), approximately 5X as much S-1 was required to achieve potentiation (i.e., ATPase rates exceeding that of S1-actin alone). Significantly, similar results were obtained when the NPTM and TM concentrations were increased 7 fold, from 1.14 μM to 8 μM. Thus the present observations cannot be ascribed to incomplete saturation of the F-actin. In terms of the two state binding model for the attachment of myosin heads to regulated F-actin, these results suggest that when the overlap region of TM is intact, more regulatory units are intrinsically in the strong S-1 binding form (supported by the Alberta Heritage for Medical Research and the Medical Research Council of Canada).

W-AM-F1 RAPID COOLING CONTRACTURES IN CARDIAC MUSCLE REFLECT SR Ca DEPLETION AND REFILLING. **By Donald M. Bers, Division of Biomedical Sciences, University of California, Riverside, CA 92521.**
The influence of rest periods on twitches (T) and rapid cooling contractures (RCCs) was studied in rabbit, rat, guinea-pig and frog ventricle (V) and rabbit atrium (At). RCCs were used as a relative index of SR Ca content. After increasing rest periods, rabbit and guinea-pig V exhibit a decline of both twitch force and RCC force (rest decay). When stimulation is resumed, T and RCCs recover. The SR (and cells) in these tissues may lose Ca during quiescence and then become reloaded again with progressive stimulation. Frog V exhibited rest decay of twitch tension, but only small RCCs which declined only slightly as a function of rest duration. Rat V and rabbit At exhibited an increase in both twitch and RCC tension as a function of rest duration (rest potentiation). Resumption of stimulation resulted in parallel declines of both twitch and RCC tension with both values approaching a steady state. These results suggest that stimulation in rat V and rabbit At may lead to a net Ca loss from the SR (and the cell) and quiescence may lead to replenishment of cellular Ca. This major functional difference in Ca metabolism in mammalian cardiac muscles might be due to a fundamental difference in SR properties, but may alternatively be due to differences in sarcolemmal transport properties or a combination thereof. After long rest intervals in rabbit and guinea-pig ventricle RCCs return toward their steady state value after considerably fewer beats than required for twitch tension. This implies that something other than SR refilling is responsible for the slow phase of twitch recovery after long rests. In rabbit ventricle increasing frequency or $[Ca]_o$ generally lead to increases in both twitch and RCC tension. However, decreasing $[Ca]_o$ (to 0.2 mM) does not decrease RCCs much despite a dramatic decline in twitch tension. This suggests that at low $[Ca]_o$ twitch tension is small despite a loaded SR.

W-AM-F2 THE INFLUENCE OF TEMPERATURE ON THE CALCIUM SENSITIVITY OF SKINNED VENTRICULAR MUSCLE FROM THE RABBIT **by Simon M. Harrison and Donald M. Bers, Division of Biomedical Sciences, University of California, Riverside, CA 92521-0121, U.S.A.**

The steady-state myofilament Ca-sensitivity was determined in skinned cardiac trabeculae from the rabbit right ventricle (diam .18-.35mm) at 36, 29, 22, 15, 8 and 1°C. Muscles were stimulated at 0.5Hz and stretched to a length which generated maximum twitch tension. The preparation was then skinned with 1% v/v Triton X-100 in relaxing medium (pCa 9.0). Each preparation was exposed to a range of Ca-containing solutions (pCa 6.5 - 4.0) at two of the six temperatures studied (e.g. 36 and 29, or 22 and 15, or 8 and 1°C). Separate solutions were made for each temperature due to the temperature sensitivity of calcium and proton binding to EGTA and Hepes, respectively. Temperature was regulated to ± 0.1°C. The pCas (mean ± SEM, n=6) generating half maximal tension at 36, 29, 22, 15, 8 and 1°C were 5.47 ± 0.03 , 5.49 ± 0.03, 5.34 ± 0.02, 5.26 ± 0.04, 4.93 ± 0.02 and 4.73 ± 0.02, respectively. The Maximum tension (C_{max}) developed by the preparation as a percentage of that at 22°C was 118, 108, 74, 57 and 29% at 36, 29, 15, 8 and 1°C, respectively. The figure shows mean Ca-sensitivity curves (C_{max} at each temperature as % of C_{max} at 22°C) for 36, 22 and 1°C. As cooling led to a shift of Ca-sensitivity towards higher $[Ca^{2+}]$ and a reduction of C_{max}, the curves do not cross over as has been described for canine Purkinje tissue (Fabiato 1985, J.Gen Physiol, 85, 247-289) or frog skeletal muscle (Godt and Lindley 1982, J.Gen Physiol. 80, 279-297).

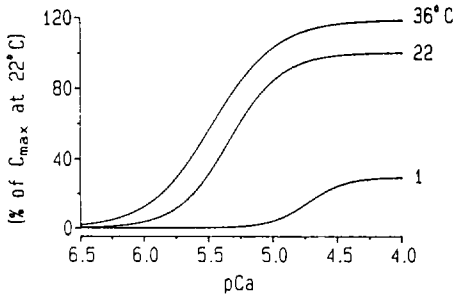

W-AM-F3 RAPID REWARMING OF CARDIAC MUSCLE DURING RAPID COOLING CONTRACTURES SUGGEST SPECIES DIFFERENCES IN MYOFILAMENT Ca SENSITIVITY. **By Donald M. Bers and Simon M. Harrison. Division of Biomedical Sciences, University of California, Riverside CA 92521.**

Rapid cooling contractures (RCCs) in intact mammalian cardiac muscle provide a useful index of SR Ca content. It is believed that cooling from 30°C to 1°C causes SR Ca to be released into the sarcoplasm and since the cold inhibits Ca pumps, $[Ca]_i$ rises, producing a contracture. When rabbit ventricular muscle is rapidly rewarmed during an RCC, tension rises transiently, followed by relaxation and we call this a rewarming spike. This rewarming spike can be explained by an increase in myofilament Ca sensitivity upon warming, followed by re-activation of processes which lower sarcoplasmic [Ca] (e.g. SR Ca-pump). In rabbit and rat ventricle and rabbit atrium, rewarming spikes are observed at all levels of tension. This implies that warming shifts the pCa vs. tension relation of the myofilaments to higher tension at all [Ca] (i.e. no crossover). This conclusion is supported by experiments with chemically skinned rabbit ventricular muscle (Harrison and Bers, Biophys. J. abstract, this issue). In contrast, rewarming spikes are only observed in frog and guinea-pig ventricle when the level of force in the cold is relatively high (i.e. at lower levels of force during an RCC, rewarming causes only relaxation and hence no spike). These results suggest that in frog and guinea-pig ventricle the pCa vs. tension curves at 30° and 1°C cross as in frog skeletal muscle (Godt and Lindley, J. Gen. Physiol. 80: 279-297, 1982; Stephenson and Williams, J. Physiol. 360: 1-12, 1985). Thus, rewarming at a $[Ca]_i$ above the crossover point leads to an increase in force, while rewarming at lower $[Ca]_i$ leads to a decrease in force. It may be anticipated that cooling reduces maximum developed force in all the cardiac tissues studied. However, myofilament Ca sensitivity is reduced by cooling in rabbit ventricle and atrium and rat ventricle, but increased by cooling in guinea pig and frog ventricle. This suggests a fundamental difference in thermodynamic properties of cardiac myofilaments of different species.

W-AM-F4 **SR Ca-PUMP AND SARCOLEMMAL Na-Ca EXCHANGE IN RELAXATION OF CARDIAC MUSCLE WITH AND WITHOUT RYANODINE.** By Donald M. Bers, Division of Biomedical Sciences, University of California, Riverside, CA 92521.

Relaxation was studied during rapid rewarming of rabbit ventricular muscles which had been activated by rapid cooling. Rewarming from 1°C to 30°C (in < 0.5 sec) activates mechanisms which contribute to the reduction of $[Ca]_i$ and thus relaxation (e.g. SR Ca-pump, sarcolemmal Na-Ca exchange and Ca-pump). Rapid rewarming in normal Tyrode (NT) induces relaxation in < 1 sec ($t_{\frac{1}{2}}$=0.23 sec). During cold exposure, changing the superfusate to a Na-free, Ca-free medium with 2 mM $CoCl_2$ (**0 Na**) does not slow relaxation upon rewarming in the same medium ($t_{\frac{1}{2}}$=0.21 sec). Addition of 10 mM caffeine to NT during cold superfusion slows relaxation somewhat (**Caff**, $t_{\frac{1}{2}}$=0.58). However, if both interventions are combined (**0 Na + Caff**) during the cold exposure, the rewarming relaxation is greatly slowed ($t_{\frac{1}{2}}$=2 sec). These results suggest that either the SR Ca-pump or, to a lesser extent, sarcolemmal Na-Ca exchange can produce rapid relaxation, but if both systems are blocked relaxation is very slow. If muscles are equilibrated with 500 nM ryanodine (Ry) prior to cooling, relaxation upon rewarming is not slowed ($t_{\frac{1}{2}}$=0.22 sec) even if Na-free, Ca-free with $CoCl_2$ solution is applied during the cold and rewarming ($t_{\frac{1}{2}}$=0.21 sec). The figure shows relaxation timecourses for the conditions described. The curves for Ry and 0Na ± Ry are superimposable with the NT curve. This result suggests that ryanodine does not prevent the SR from accumulating Ca to produce relaxation.

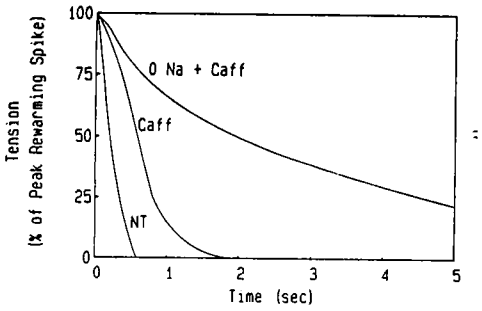

W-AM-F5 A COMPARISON OF THE EFFECTS OF MYOFILAMENT SPACE [Ca] AND [Ba] ON Ca RELEASE RATES FROM THE SARCOPLASMIC RETICULUM. Wai-Meng Kwok and Philip M. Best, Dept. of Physiology & Biophysics, Univ. of Illinois, Urbana, IL 61801.

Intracellular Ca ion is known to modulate Ca channel function in numerous excitable cells, while intracellular Ba does not have pronounced effects. We have previously investigated the effect of myofilament space [Ca] on Ca release rates from the sarcoplasmic reticulum (SR) of skinned (sarcolemma removed), skeletal muscle fibers. We observed a Ca dependent inactivation of Ca release for myofilament space [Ca] between pCa=5.8 and 7 (Biophys. J. 51, 104a, 1987). We now report that the observed Ca inactivation was not due to a decrease in the driving force for Ca across the SR membrane. Furthermore, the effect of varying [Ba] in the myofilament space on SR Ca release was investigated. Ca release rates were measured optically with 0.4mM antipyrylazo III. The solutions contained 2mM MgATP, 15mM CP, 1mM Mg, 100mM monovalent cations, about 35mM MOPS buffer (pH=7 at 10°C), and variable pCa and pBa; I=0.15. Following a standard loading procedure, Ca release was stimulated by exposing fibers to 7.5mM caffeine. A Ca release rate in the test solution was obtained and compared to the average of two bracketing control release rates. Control solutions contained pBa=8 and test solutions contained either pBa=5, 6.5 or 6.8, the range over which Ca caused maximum inhibition. No major inhibition of Ca release was found with any pBa. The % of control Ca release rates for pBa=6, 6.5, and 6.8 were (mean ± s.e.m.) 99±4 (n=7), 97±4 (n=19) and 88±4 (n=12) respectively. Hence, unlike elevated myofilament space Ca which causes significant inhibition of Ca release, myofilament space Ba does not affect the rate of SR calcium release appreciably. This aspect of the SR Ca channel is similar to that of Ca channels found in the surface membranes of some excitable cells. Supported by NIH AR32062 (PMB)

W-AM-F6 SODIUM-CALCIUM EXCHANGE CAN MEDIATE VOLTAGE DEPENDENT RELAXATION IN GUINEA PIG VENTRICULAR MYOCYTES. John H.B. Bridge and Kenneth W. Spitzer, Nora Eccles Harrison CVRTI, University of Utah, Salt Lake City, Utah 84112

We investigated the hypothesis that in heart cells in which the SR is paralyzed with caffeine (10.0 mM) a voltage sensitive Na/Ca exchange might underly voltage sensitive mechanical relaxation. We used suction micro-electrodes and a discontinuous voltage clamp circuit to control membrane potential in guinea pig ventricular myocytes. A video monitor system was used to measure cell shortening. Cells were superfused with a bicarbonate buffered modified Tyrode solution containing 2.7 mM Ca. Voltage clamp pulses (5 secs duration, -80 to +10 mV) produced an initial phasic contraction and relaxation followed by tonic shortening. Complete relaxation occurred upon repolarization to -80 mV. In the presence of 10.0 mM caffeine the phasic component of contraction disappeared and enlarged tonic contractions remained which only relaxed upon repolarization to -80 mV. The rate of relaxation depended steeply upon the voltage at which it occurred and approximately doubled between -40 and -80 mV. The rate of relaxation at -80 mV was significantly slowed when $[Na]_o$ was reduced to 70 mM (Li replacement). However, the relaxation rate could be restored to that which occurred in normal Na_o (-80 mV) by hyperpolarizing the cell to -140 mV. Moreover, while reduction of $[Na]_o$ to 70 mM slowed relaxation simultaneous reduction of $[Ca]_o$ to 80 µM restored the relaxation rate. This latter finding indicates a competitive effect of Na_o and Ca_o on relaxation in the presence of caffeine. The effect of Na and Ca on relaxation rate suggest the involvement of Na/Ca exchange under these circumstances. We infer that in the presence of caffeine (which prevents SR sequestration) mechanical relaxation is produced when a voltage sensitive Na/Ca exchange removes Ca from the cytosol.

W-AM-F7 Steady-State Tension-$[Ca^{2+}]$ Relationship in Intact Human Myocardium. Judith K. Gwathmey and Roger J. Hajjar. Beth Israel Hospital and Harvard Medical School, Boston, Ma.
Steady contractile activation was achieved by stimulating (15-25 Hz) intact human trabeculae, loaded with aequorin, a Ca^{2+}-sensitive bioluminescent protein. Steady force and intracellular $[Ca^{2+}]$ were measured during the tetani and a tension vs. $[Ca^{2+}]_i$ relationship was obtained by varying the $[Ca^{2+}]_o$ concentration. Since many investigators have made inferences about the sensitivity of the myofilaments using the peak force vs. peak $[Ca^{2+}]_i$ relationship from twitches, we compared it to the steady-state force-$[Ca^{2+}]_i$ relationship obtained from tetani. Both relationships were described by the Hill equation: %Tension = $[Ca^{2+}]_i^n/(Q+[Ca^{2+}]_i^n)$, where the Hill coefficient, n, is an index of the steepness of the curve, and Q is an affinity constant. The curve of tetani had a Hill coefficient of 5.1 and a half-maximal $[Ca^{2+}]$ ($[Ca^{2+}]_{50\%}$) was 5.3×10^{-6}M, whereas the curve from twitches was shallower with n = 3.7 and shifted to the right with $[Ca^{2+}]_{50\%}$ = 1.6×10^{-6}M. Changes in the steady-state force-$[Ca^{2+}]_i$ was correlated with alterations in the sensitivity of the myofilaments to Ca^{2+}, whereas changes in the peak force-peak $[Ca^{2+}]_i$ relationship was correlated with the time course of the calcium transient. Agents that increased the time course of the calcium (and twitch) transient shifted the peak-force vs. peak $[Ca^{2+}]_i$ relation to the left whereas agents that increased the sensitivity of the myofilaments to Ca^{2+} displaced both the twitch curve and tetanus curve to the left. This leads us to the conclusion that peak force-peak $[Ca^{2+}]_i$ can not be used to estimate sensitivity changes at the level of the myofilaments. Support:HL39091 and Biomedical Resarch Grant Beth Israel Hospital.

W-AM-F8 CHANGES IN MYOPLASMIC FREE $[Ca^{2+}]$ WITH AGING. V. Sanchez[1], J.R. López[1], M. Mendoza[1] and F.A. Sréter[2], [1]Centro de Biofísica y Bioquímica, Instituto Venezolano de Investigaciones Científicas, Apartado 1827, Caracas, Venezuela; [2]Department of Anesthesia, Massachusetts General Hospital and Harvard Medical School, and Department of Muscle Research, Boston Biomedical Research Institute, Boston, MA 02114.

Previous work has shown that the activity of several membrane enzymes decreases with age (Grinna and Barber, *Biochim. Biophys. Acta,* **288**:347, 1972). The intracellular calcium homeostasis in skeletal muscle involves calcium transport systems located in the sarcolemma and in the sarcoplasmic reticulum which are either coupled to the hydrolysis of ATP or modulated by ATP. We have measured the intracellular free calcium concentration ($[Ca^{2+}]_i$) in skeletal muscle fibers isolated from rats of different ages. Sprague-Dawley and Wistar rats aged 6 months (young), 12 months (adult) and 24 months (old) of age were deeply anesthetized after which the extensor digitorum longus (EDL) was dissected and placed in an experimental chamber for electrophysiological measurements. $[Ca^{2+}]_i$ was determined by means of Ca^{2+}-selective microelectrodes which were prepared and calibrated as previously described (Lopez, et al., *Biophys. J.*, **43**:1, 1983). The mean resting $[Ca^{2+}]_i$ in the young rats was 0.12 ± 0.01 μM (mean ± SEM), in the adult rats was 0.15 ± 0.02 μM, and in the old rats was 0.35 ± 0.02 μM. We did not observe any detectable difference in the resting membrane potential among the three groups of rats. These results show clearly that there is a significant difference in $[Ca^{2+}]_i$ between young and adult rats in comparison to old rats. [Supported by grants from MDA and CONICIT of Venezuela S1-1277 to JRL and NIH Center Grant GM15904 to the Department of Anesthesia].

W-AM-F9 TWO STRUCTURALLY DISTINCT CALCIUM STORAGE SITES IN RAT CARDIAC SARCOPLASMIC RETICULUM. A.O. Jorgensen*, R. Broderick**, A.P. Somlyo** & A.V. Somlyo**, *Dept. of Anatomy, Univ. of Toronto, Toronto, Canada. **Penn. Muscle Inst., Univ. of Penn., Philadelphia, PA, USA.

The elemental composition of subcellular organelles in relaxed rat papillary muscle was measured by electron probe x-ray microanalysis of cryosections of flash-frozen tissue. Calsequestrin was localized by immunoelectron microscopy. Non-mitochondrial electron dense structures (50 to 150 nm in diameter) with a [P]>375 mmoles/kg dry wt were identified in the interfibrillar spaces of the I-band region. They were not visibly associated with transverse tubules. The Na, Mg, P, S, Cl and K contents of the electron dense structures were normally distributed consistent with the uniform composition of a specific subcellular organelle, but the distribution of the calcium concentrations {in these electron dense structures} was bimodal. One population had a relatively high [Ca] (up to 53 mmoles/kg dry wt) content with a mean mmoles/kg dry wt ± S.E.M. of 10.5 ± 0.5 while the other one had a relatively low [Ca] with a mean value of 2.8 ± 0.3. The mean [Ca] in the junctional SR (j-SR) in rat papillary muscle with [Ca]>6 was 14.6 ± 2.0. We propose that the electron dense structures described above correspond to non-junctional sarcoplasmic reticulum and that the population containing relatively high [Ca] is the calsequestrin containing corbular SR (c-SR) confined to the I-band region, while the population containing relatively low [Ca] corresponds to anastomosing regions of the network SR that lack calsequestrin. These results are consistent with the idea that both the c-SR and the j-SR are potential sources of and/or sinks for Ca^{2+} released into the myofibrillar space during excitation-contraction coupling in cardiac muscle. Supported by HL 15 835 to PMI and by HSFO T455 to AOJ.

W-AM-F10 CHARACTERIZATION OF PROTEINS INCOLVED IN EXCITATION_CONTRACTION COUPLING IN MICE WITH MUSCULAR DYSGENESIS. C. Michael Knudson[+], Nirupa Chaudhari[*], Kurt G. Beam[*], and Kevin P. Campbell[+]. [+]Dept. of Physiology and Biophysics, University of Iowa, Iowa City, IA 52242 and [*]Dept. of Physiology, Colorado State University, Fort Collins, CO 80523.

Recent results from our laboratory (Imagawa et al., JBC in press) suggest that the ryanodine receptor is the calcium release channel of the sarcoplasmic reticulum (SR) while the results of Rios et al. (Nature 325:717, 1987) suggest the dihydropyridine (DHP) receptor may couple depolarization of the transverse tubules to calcium release from the SR. Muscular Dysgenesis (mdg) is a lethal autosomal recessive trait in mice which manifests as a failure of excitation-contraction (E-C) coupling. Previous work has shown that dysgenic muscle homogenates have an 80% reduction in high affinity DHP binding and completely lack the DHP-sensitive calcium current. Our goal is to determine if the lack of E-C coupling in dysgenic muscle is the result of a mutated calcium channel/DHP receptor of the transverse tubules or if the mutated gene codes for a junctional SR protein which secondarily affects the calcium channel/DHP receptor. To determine the cause of these deficits in dysgenic muscle we have examined skeletal muscle extracts from control and mdg mice for various protein components of E-C coupling. Extracts were run on SDS-PAGE gels and transferred to nitrocellulose for analysis using monoclonal antibodies directed against calsequestrin and the 170 kDa DHP binding subunit of the DHP receptor. Initial results show that calsequestrin is detected on immunoblots in roughly equal quantities for both control and dysgenic mice while the 170 kDa subunit of the DHP receptor was not detected on immunoblots of dysgenic extracts. These results suggest that the reduced DHP binding in mdg mice may be due to the lack of the DHP binding subunit of the receptor. (Supported by NIH HL 37187)

W-AM-F11 Dysfunction of $[Ca^{2+}]_i$ in Duchenne Muscular Dystrophy fibers. V. Sánchez[1], J. R. López[1], L. E. Briceño[2], [1]Centro de Biofísica y Bioquímica, Instituto Venezolano de Investigaciones Científicas, Apart. 21827 Caracas, Venezuela. [2]Dept. de Neurología Hospital J. M. de los Ríos, Caracas, Venezuela.

Abnormal accumulation of calcium at the myoplasm has been associated with Duchenne Muscular Dystrophy (DMD). We have shown that the myoplasmic $[Ca^{2+}]$ is 3.9, times higher in Dystrophic hamster than control (Biophys. J. 51:551a 1986). We have extendended previous studies by measuring $[Ca^{2+}]_i$ by means of Ca^{2+} selective microelectrodes in intact intercostal muscle fibers isolated from DMD patients and from subjects with no evidence of neuromuscular disease, who served as controls. The Ca^{2+} selective microelectrodes were prepared and calibrated as described previously (López et al Biophy J. 43:1, 1983). The mean resting membrane potential and $[Ca^{2+}]_i$ were -83 $\pm$ 1 mV (M $\pm$ SEM) and 0.10 $\pm$ 0.01 μM (M $\pm$ SEM) in the control subjects. On the other hand, similar determinations carrier out in DMD muscle fibers showed a mean value of -76 $\pm$ 1 mV (M $\pm$ SEM) and 0.36 $\pm$ 0.02 μM (M $\pm$ SEM) for the resting membrane potential and $[Ca^{2+}]_i$ respectively. This dysfunction in the regulation of myoplasmic $[Ca^{2+}]_i$ might be linked to the protein degradation mediated by the Ca^{2+} dependend proteases thus leading to necrosis of the muscle fibers. (Supported by Muscular Dystrophy Association (MDA), Conicit S1-1277, and Elmor of Venezuela).

W-AM-G1 EXPRESSION AND SITE-DIRECTED MUTATION ANALYSIS OF BACTERIO-OPSIN. M. Betlach, L. Miercke, R. Shand, A. Mitra, and R. Stroud. Department of Biochemistry and Biophysics, University of California, San Francisco, CA 94143-0448.

An efficient E. coli expression vector has been constructed for bacterio-opsin. In a crude lysate from nine liters of E. coli cells harboring the expression vector, bacterio-opsin levels assayed immunologically are approx. 200 mg which constitutes 7.8% of the total protein. This bacterio-opsin made in E. coli (e-BO) has been localized to the E. coli cytoplasmic membrane. Throughout purification steps following pelleting and solubilization of the crude membrane fraction, e-BO can be successfully regenerated with retinal and synthetic lipids. Site directed mutations have been introduced using the single-stranded phage M13 system and the Kunkel method (PNAS 82, 488-492, 1985) which enables an effective selection against the wild type unmutagenized strand.

W-AM-G2 STUDIES OF MULTIPLE ISOELECTRIC FORMS OF BACTERIORHODOPSIN. P.E. Ross, S.L. Helgerson, L.J.W. Miercke* and E.A. Dratz, Dept. of Chemistry, Montana State University, Bozeman, MT 59717; *Dept. of Biochemistry and Biophysics, University of California, San Francisco, CA 94143.

Multiple isoelectric forms of bacteriorhodopsin (bR) are found in immobilized pH gradient gels. Detergent solubilized bR focuses into five doublet bands at isoelectric points (pI) 4.9, 5.0, 5.2, 5.5 and 5.6 detected by a silver staining procedure. We are exploring the origins of the doublet bands from purple membrane (pm). They include the presence of bR precursor proteins and non-bR proteins. Before staining, the principal doublet at pI 5.2 is visible by its purple color. Narrowing the pH gradient shows that the principal doublet contains bands at pI 5.20 and 5.24. Both of the unstained bands have a λmax = 550 nm, consistent with the absorbance maximum of detergent solubilized bR. The ratio of absorbance of the two components ranges from 1.7-2.0 (pI 5.20/pI 5.24). To characterize these isoelectric species further, native pm was proteolyzed with papain. Papain produces a two-step cleavage of carboxyl tail residues. The first cleavage is proposed to occur between residues 239 and 240 which removes Asp-242, while the second cleavage between residues 231 and 232 removes Glu-232, 234 and 237 (1). The shift in pI to 5.5 observed for the first cleavage (+0.3 pH units) is associated with the loss of a single negative charge. The pI shift to 6.1 (+0.6 pH units) which occurs with the second cleavage is therefore consistent with the loss of two negative charges. This is supported by carbodiimide-mediated labeling experiments which suggest at least one of the Glu residues is protonated (1). These results show a shift in the pI of 0.3 pH per negatively charged group.(Support NIH R01 EY-6914; ONR N00014-87-K-0278)
(1) R. Renthal, N. Dawson, J. Tuley and P. Horowitz (1983) Biochemistry 22:5.

W-AM-G3 A CATION BINDING SITE IN BACTERIORHODOPSIN PREDICTED FROM THE PRIMARY SEQUENCE. S.L. Helgerson and E.A. Dratz, Dept. of Chemistry, Montana State Univ., Bozeman, MT 59717.

Bacteriorhodopsin (bR) is the major protein in the purple membrane (pm) of H. halobium. Native bR in pm absorbs light at λmax = 570 nm, but shifts to λmax > 600 nm to form blue membrane (bm) when all cations are removed. Deionized bR in bm has an altered photocycle and apparently does not function as a proton pump. Addition of cations to bm restores the native pm color and function. Evidence for localized cation binding sites in bR has been presented based on x-ray diffraction difference maps for Pb^{+2} minus Ca^{+2} reconstituted membranes (1). We find using primary sequence and secondary structure analyses that a cation binding site may be formed by bR residues acting as calcium-ligands (x) Asp-102, (y) Asp-104, (z) Gln-105, (-y) Thr-107, and (-x) a bound water. These residues occur in a region with striking sequence homology to the calcium-ligands of the calmodulin binding site II:

```
                                  x   y   z  -y  -x   -z
                                  |   |   |   |   |    |
CaM (48-75):  L Q D M I N E V D A D G N G T I D F P E F L T M M A R K
              |   |         | | | |   | | | |
bR (94-120):  L L D L A L L V D A D   Q   G T I L A L V G A D G L M I G
```

The missing (-z) ligand could be contributed by bR residues Glu-161 or -166. The rationale for this prediction will be discussed considering known structural features of bR (2) and rules for identifying EF-hand cation binding sites (3). (Support: NIH RO1 EY-6914-02; ONR N00014-87-K-0278)
(1) N.V. Katre, Y. Kimura and R.M. Stroud (1986) Biophys. J. 50:277; (2) D.A. Agard and R.M. Stroud (1982) Biophys. J. 37:589; (3) D.M. Szebenyi and K. Moffat (1986) J. Biol. Chem. 261:8761.

W-AM-G4 SECOND HARMONIC GENERATION FROM LANGMUIR BLODGETT FILMS OF RETINAL, RETINAL SCHIFF BASES AND PURPLE MEMBRANE J.Y. Huang*, Th. Rasing+, and A. Lewis* *Department of Applied Physics, Cornell University, Ithaca, New York. +Department of Physics, University of California, Berkeley, California.

The second harmonic generation (SHG) signal from monolayers of retinal, retinal Schiff bases, and purple membrane are reported. The results have yielded information on the monolayer structure and demonstrate that retinal and retinal Schiff bases have large second-order molecular hyperpolarizabilities. Using excitation at 532nm, hyperpolarizabilities of 1.4×10^{-28} esu, 1.2×10^{-28} esu, and 2.3×10^{-28} esu were obtained for retinal, the unprotonated Schiff base, and the protonated Schiff base respectively. These values compare well with the known variation in the alteration in the dipole moment of such chromophores upon excitation. We have extended these measurements to include a comparision of the SHG in these monolayers with data we obtained from purple membrane. Our data indicate that the hyperpolarizability in the membrane appears to be identical to that of the free protonated retinylidene Schiff base chromophore. The SHG spectrum of all-trans retinal monolayer exhibits a small one-photon forbidden peak in addition to the main absorption peak.

W-AM-G5 IN-PLANE POSITION OF THE SCHIFF'S BASE END OF THE CHROMOPHORE OF BACTERIORHODOPSIN M.P. Heyn, F. Seiff, J. Westerhausen and I. Wallat, Biophysics Group, Freie Universität Berlin, D-1000 Berlin, FRG.

In previous work retinals that were partially deuterated in the middle of the chain (1) and in the cyclohexene ring (2) were spontaneously incorporated into bacteriorhodopsin (bR) by adding them to the growth medium of the retinal-minus mutant JW5. Using the large difference in neutron cross-section between protons and deuterons, the in-plane positions of these labelled parts of the chromophore were determined by neutron diffraction (1,2). We have now completed this project by synthesizing a retinal labelled with 5 deuterons as close as possible to the Schiff's base (3 in the 13-methyl group and one each at C-14 and C-15). The position of the label was determined. Together with our previous results the following picture of the arrangement of the chromophore within bR emerges. The three labelled positions are on one line, as would be expected if the plane of the chromophore were approximately perpendicular to the plane of the membrane. On the basis of linear dichroism experiments, the angle of tilt between the polyene chain and the plane of the membrane is believed to be about 20° (3). The distances between the labelled positions are consistent with this value. Extrapolation along the line determined by the 3 label positions lead to a fairly accurate position for the Schiff's base nitrogen. We conclude that helix G to which the chromophore is attached at lys 216 can only be helix 2 or 6. Our results show that under favorable conditions it is possible to locate a small group containing as few as 5 deuteriums in a membrane protein.
(1) P.N.A.S. 82 (1985) 3227. (2) P.N.A.S. 83 (1986) 7746. (3) J. Mol. Biol. 117 (1977) 607.

W-AM-G6 **EXCHANGE OF THE BACTERIORHODOPSIN SCHIFF-BASE PROTON WITH BULK WATER** **Gerard S. Harbison, Department of Chemistry, State University of New York, Stony Brook, NY 11794; James E. Roberts, Department of Chemistry, Lehigh University, Bethlehem, PA 18015; Judith Herzfeld, Department of Chemistry, Brandeis University, Waltham, MA 02254; Robert G. Griffin, Francis Bitter National Magnet Laboratory, M.I.T., Cambridge, MA 02139.**

Using a newly devised pulse-sequence, combined with magic-angle spinning, we have been able to follow the proton exchange between bulk water and the Schiff-base proton of fully-hydrated (ϵ-^{15}N)-lysyl-bacteriorhodopsin. Our innovation is a time delay τ after the initial 90° ^{1}H pulse in the standard cross-polarisation sequence. During this delay, which can vary between 200 μs and 20 ms, the proton magnetisation of bR itself dephases rapidly as a result of the large proton-proton dipolar interactions in the essentially immobile protein. In contrast, the water proton magnetisation, which has a T_2 of the order of 50 ms, is relatvely unaffected by the time delay. Application of Hartmann-Hahn-matched spin-locks on the ^{1}H and ^{15}N nuclei preserves any of the on-resonance water proton magnetisation which may have been transferred to immobile protein residues by chemical exchange during the spin-locking period; it also cross-polarises any ^{15}N species which are directly bonded, or in close proximity, to the exchanging protons. The ^{15}N signal is then detected. The pulse sequence yields a ^{15}N spectrum in which signals are observed for the lysine amino groups, and for the Schiff-base nitrogens of both isomers of dark-adapted bR, but not for the non-exchanging peptide groups. By varying the timing of the pulse sequence we can set a lower limit for the rate of exchange of the Schiff base proton; we find that the exchange is complete within 0.5 ms, implying a time constant of 0.3 ms or less. This finding is consistent with the results of separated-local-field studies in our laboratory, and with the stopped-flow Raman data of other workers (Doukas *et al.*, Biophys. J. *33*, 275); we have however been able to extend their minimum rate upward by an order of magnitude. This fast exchange of the Schiff-base proton, at a rate comparable to those observed for nitrogen bases in free aqueous solution, indicates that there exists an efficient channel for protons between the bR chromophore and the aqueous phase.

W-AM-G7 **THE PHOTOCYCLE OF HALORHODOPSIN**, J. Tittor and D. Oesterhelt, Max-Planck-Institute for Biochemistry, 8000 Munich, West-Germany

The retinal protein halorhodopsin (HR) acts as a light-driven Cl^- pump in the plasmamembrane of *Halobacterium halobium* . Upon excitation with light a photocycle in the millisecond time range is triggered, which mediates ion translocation. Evaluation of time resolved difference spectra of the photocycle led to a cyclic reaction scheme which shows two Cl^--dependent equilibiria(1). One determines the relative amounts of the intermediates HR_{520} and HR_{640} occuring upon excitation of the initial states HR_{578} and HR_{565} which are connected via the second Cl^- equilibrium. Chloride dependency and selected time windows allowed the reduction of complex intermediate difference spectra to that of single A to B transitions. Subsequently absolute spectra were calculated which are independent from the architecture of the underlying kinetic reaction scheme. All experimentally observed absorbance changes after a light flash can be simulated by these spectra, a set of 5 rate constants and the photocycle scheme presented. The agreement of the calculated and experimental traces ones is better than 90%. This accuracy proves the correctness of the suggested photocycle scheme and gives a powerfool tool for further spectroscopic investigations on the photochemical properties of this protein under different experimental conditions.

(1)Tittor,J.,D.Oesterhelt,R.Maurer, H.Desel and R.Uhl 1987, Biophys. J. Vol 52

W-AM-G8 MEMBRANE POTENTIAL MODULATES PHOTOCYCLING RATES OF BACTERIAL RHODOPSINS IN VIVO AND IN ARTIFICIALLY ENERGIZED VESICLES. D. Manor, C.A. Hasselbacher, J.L. Spudich, Dept. of Structural Biology, A. Einstein College of Medicine, Bronx, N.Y. 10461.

We observe each of the 3 retinal proteins in Halobacterium halobium: sensory rhodopsin I (SR-I), bacteriorhodopsin (BR), and halorhodopsin (HR) exhibits a decreased rate of thermal decay of its principal intermediate when photoactivated in an artificially energized compared to de-energized membrane. This result generalizes the membrane potential modulation of the BR photocycle noted previously (Dancshazy, et al. (1983) Photobiochem. Photobiophys. 5, 347), and an effect on SR-I suggested earlier by the observation that the SR-I photocycle was retarded by photoactivation of HR in the same membrane (R.A. Bogomolni, personal communication). SR-I photochemical reactions were measured in phototactic H. halobium cells, and differences from vesicle photocycle kinetics are attributable to the electrical membrane potential present in the cells. The thermal return of S_{373} to $SR\text{-}I_{587}$ in vesicles occurs at nearly twice the in vivo rate ($t_{50\%}$ = 1.2 sec in intact cells and 0.7 sec in cell envelopes). S_{373} decay in vivo is biphasic ($t_{50\%\ slow}$ = 1.0 sec, $t_{50\%\ fast}$ = 0.3 sec) rather than monophasic as in vesicles. HR differs from BR and SR-I in that HR_{520} decay is monophasic at all membrane potential values tested (-100 to 0 mV). In vivo SR-I photocycling rates were reproduced in envelope vesicle preparations in the presence of valinomycin-induced potassium diffusion potentials.

W-AM-G9 FLUORESCENCE EMISSION IN THE K INTERMEDIATE OF THE BR PHOTOCYCLE--D. Blanchard, H. Lemaire, T. Brack, H. Hayashi and G. H. Atkinson

The purple membrane of Halobacterium halobrium containing the protein bacteriorhodopsin (BR) functions as a light driven proton pump. The movement of protons from the inner to the outer part of the cell enables the cell to derive chemical free energy via the ADP to ATP conversion.

The proton pumping is accomplished through a photocycle involving the isomerization of the retinal chromophore of the protein. Only the primary events occurring in the first few picoseconds of the 5 ms photocycle are light driven. The remainder of the cycle continues thermally after the initial optical excitation.

Picosecond time-resolved fluorescence spectroscopy (PTRF) and picosecond transient absorption (PTA) are used here to monitor the electronic changes and the kinetic mechanism which occur following optical excitation. A two laser, pump-probe configuration utilizing an actively mode-locked cw Nd:YAG laser to synchronously pump two cavity dumped dye lasers is designed to record PTRF and PTA spectra. Fluorescence spectrum of a distinct isomeric and conformational intermediate, K, has been recorded over the initial 100 ps. This is the first reported fluorescence spectrum of K. This unstructured K fluorescence spectrum appears in the same region as that assigned to BR itself. It can be distinguished from the fluorescence spectrum assigned to BR by a larger emission quantum yield (twice that of BR) and by a maximum intensity shifted to higher energy from the maximum of BR fluorescence spectrum.

W-AM-G10 PICOSECOND INTERMEDIATES IN THE BACTERIORHODOPSIN PHOTOCYCLE--T. L. Brack, H. Hayashi, D. Blanchard, and G. H. Atkinson

The purple membrane of Halobacterium halobrium containing the protein, bacteriorhodopsin (BR), functions as a light driven proton pump transporting protons from inside to outside of the cell enabling the cell to store this light derived chemical free energy via its normal ADP to ATP conversion mechanisms.

The proton pumping is accomplished through a photocycle involving the isomerization of the retinal chromophore of the protein. Only the primary events occurring in the first few picoseconds of the 5 millisecond photocycle are light driven. The remainder of the cycle continues thermally after the initial optical excitation.

Picosecond time-resolved resonance Raman spectroscopy (PTR^3) is used here to obtain vibrational spectra which provide information on the structure and conformation of the retinal chromophore during the initial 100 ps of the BR photocycle. A two laser, pump-probe configuration utilizing an actively mode-locked, cw Nd:YAG laser to synchronously pump two cavity dumped dye lasers is designed to record PTR^3 spectra. Several molecular motions within the retinal chromophore, formulated in terms of a normal coordinate approximation, have been monitored by PTR^3 spectroscopy over the initial 100 ps interval. These molecular motions characterize the overall conformational and structural changes in retinal occurring on the picosecond time scale. The vibrational Raman spectra of the prompt intermediate formed during the laser pulsewidth is different from that of intermediate(s) observed later during the first 100 ps following photoinitation of the cycle. These PTR^3 data are correlated to obtain a model describing the molecular dynamics and photophysics of retinal during the first 100 ps of the BR photocycle.

W-AM-G11 BACTERIORHODOPSIN'S L_{550} INTERMEDIATE CONTAINS A C_{14}-C_{15} S-*TRANS* RETINAL CHROMOPHORE. Stephen P. A. Fodor, Walter T. Pollard, Richard A. Mathies, Dept. of Chemistry, Univ. of Calif., Berkeley, CA 94720; R. Gebhard, E. van den Berg and Johan Lugtenburg, Dept. of Chemistry, Leiden University, 2300 RA Leiden, The Netherlands.

Detailed models for the mechanism of light-driven proton transport in bacteriorhodopsin have incorporated conformational changes in the retinal C_{14}-C_{15} bond. We have determined the C_{14}-C_{15} conformation in bacteriorhodopsin's L_{550} intermediate by examining the resonance Raman spectra of bacteriorhodopsin regenerated with 14,15-dideuterio retinals. Vibrational calculations show that the C_{14}-^2H and C_{15}-^2H rocks form symmetric (A) and antisymmetric (B) combinations in the 14,15-^2H labeled chromophores. In the s-*trans* conformation, there is a small frequency separation or splitting between the A and B modes which are found at ~970cm^{-1} near the monodeuterio frequencies. In the 14-s-*cis* case, the splitting is large and the Raman active symmetric A mode is predicted at ~850 cm^{-1}. In addition, the C_{14}-^2H monodeuterio rock should appear at an unusually low frequency (920-930 cm^{-1}) in the 14-s-*cis* molecules. The vibrational calculations also indicate that conformational distortion and increased π-electron delocalization do not alter this basic pattern. Time-resolved resonance Raman spectra were obtained of bacteriorhodopsin's L_{550} intermediate containing the 14-^2H, 15-^2H and 14,15-^2H retinal derivatives. The symmetric A rock in L_{550} is found at 968 cm^{-1}, within 4 cm^{-1} of the monodeuterio frequencies. The deuterated rock frequencies of L_{550} are all found within 5 cm^{-1} of those observed in BR_{568} which contains a 14-s-*trans* chromophore. These results show that L_{550} contains a 14-s-*trans* chromophore and suggest that only 14-s-*trans* structures are involved in the proton pumping photocycle of bacteriorhodopsin.

W-AM-G12 **TYROSINE-185 ACTS AS A PROTON ACCEPTOR DURING BACTERIORHODOPSIN'S PHOTOCYCLE: EVIDENCE FROM FT-IR SPECTRA OF SITE-DIRECTED MUTANTS**

*M. S. Braiman**†, *T. Mogi**, *L. J. Stern**, *N. R. Hackett**, *H. G. Khorana**, *and K. J. Rothschild*†. *From the* **Departments of Chemistry and Biology, MIT, Cambridge, MA 02139 and the* †*Physics Department, Boston University, Boston, MA 02215.*

FT-IR difference spectroscopy of site-directed mutants has been used to investigate the role of individual tyrosine side chains in the proton-pumping mechanism of bacteriorhodopsin (bR). For each of the 11 possible bR mutants containing a single Tyr→Phe substitution, difference spectra have been obtained of the bR→K and bR→M photoreactions. Only the Tyr185→Phe mutation results in the disappearance of bands previously ascribed to the protonation of a tyrosinate side chain during the bR→K photoreaction on the basis of uniform isotope labeling of all 11 tyrosines [Rothschild *et al.* (1986) *Proc. Natl. Acad. Sci. USA* 83, 347]. The site-directed mutants now show that the particular residue involved is Tyr185. The Tyr185→Phe mutation also eliminates a set of bands in the bR→M difference spectrum associated with *deprotonation* of a Tyr; most of these bands (e.g., positive 1271- cm^{-1} peak) are completely unaffected by the other 10 Tyr→Phe mutations. Thus tyrosinate-185 gains a proton during the bR→K reaction, and loses it again when M is formed. Our FT-IR spectra also provide evidence that Tyr185 interacts closely with the protonated Schiff's base linkage of the retinal chromophore, since the negative C=NH+ stretch band shifts from 1640 in the wild type to 1636 cm^{-1} in the Tyr185→Phe mutant. A model which is consistent with these results is that Tyr185 is normally ionized and serves as a counterion to the protonated Schiff's base, and that the primary photoisomerization of the chromophore translocates the Schiff's base away from Tyr185, thereby raising its pK_a and resulting in its (transient) protonation. ***Supported by grants from the O.N.R., N.I.H., and N.S.F. M.S.B. is a Lucille P. Markey Scholar and his work was supported in part by a Lucille P. Markey Scholar Award.***

W-AM-G13 SOLID-STATE ^{13}C-NMR OF THE M_{412} PHOTOINTERMEDIATE OF BACTERIORHODOPSIN+

S.O. Smith*, J. Courtin&, E. van den Berg&, C. Winkel&, J. Lugtenburg&, J. Herzfeld#, and R.G. Griffin* *Francis Bitter National Magnet Laboratory, M.I.T., Cambridge, MA 02139; &Department of Chemistry, Rijksuniversiteit te Leiden, 2300 RA Leiden, The Netherlands, and #Department of Chemistry, Brandeis University, Waltham, MA 02254.

Solid-state ^{13}C-NMR spectra have been obtained of the M_{412} photointermediate of bacteriorhodopsin (bR) using purple membrane regenerated with retinal specifically ^{13}C-labeled at positions 5, 12, 13, 14 and 15. The M_{412} intermediate was trapped at -40°C at pH 10 in either 100 mM NaCl or 500 mM guanidine hydrochloride (G-HCl). The ^{13}C-5 resonance was observed at 139.4 ppm. The ^{13}C-5 chemical shift is consistent with a 6-s-trans structure and a negative protein charge localized near C-5 as was observed in dark-adapted bR. The ~5 ppm upfield shift of the M_{412} resonance relative to dark-adapted bR is attributed to an unprotonated Schiff base in M_{412}. The ^{13}C-12 chemical shift (128.2 ppm) indicates that the C_{13}=C_{14} double bond has a cis configuration, while the ^{13}C-13 chemical shift (146.7 ppm) demonstrates that the Schiff base is unprotonated. Of particular interest are the results of ^{13}C-14 retinal M_{412}. In 100 mM NaCl, a dramatic upfield shift was observed for the ^{13}C-14 M_{412} resonance (115.2 ppm) relative to unprotonated Schiff base model compounds (~128 ppm). In contrast, in 500 mM G-HCl the ^{13}C-14 resonance was observed at 126 ppm. The different ^{13}C-14 chemical shifts in the two M spectra may be explained by different C=N configurations in the two M preparations, <u>syn</u> in NaCl and <u>anti</u> in G-HCl. Spectra obtained of M_{412} containing ^{13}C-labeled tyrosine will also be discussed.